Methodologies for abundance estimation of moose (Alces alces) and other rare species

A Thesis

Presented to the Faculty of the Graduate School

of Cornell University

in Partial Fulfillment of the Requirements for the Degree of

Master of Science

by

Alec Wong

December 2018

ABSTRACT

Moose (*Alces alces*) are a species of management concern in New York State. In some New England states, moose populations are known to be in decline due to mortality from parasitic infection, thermal stress, nutritional deficiency, and moose-vehicle collisions. In contrast, the status of the New York moose population has not been described satisfactorily; abundance has increased since the species' recolonization in 1980, but indices of abundance such as moose-vehicle collisions and public sightings do not reflect the growth of other northeastern U.S. states. In 2015, The New York State Department of Environmental Conservation initiated the project described herein to examine aspects of this population of moose, most notably the size of the population. This thesis offers (a) an advancement of spatial capture-recapture (SCR) methodology to quantify the abundance of rare species through the integration of adaptive sampling principles, and (b) an alternative solution to SCR that estimates population size from scat collections made by detection dogs, without knowledge of individual identity.

Rare species present challenges to data collection, particularly when the species is spatially clustered over large areas, such that the encounter frequency of the organism is low. Sampling where the organism is absent consumes resources, and offers relatively low-quality information which are often difficult to model using standard statistical methods. In adaptive sampling, a probabilistic sampling method is employed first, and additional effort is allocated in the vicinity of sites where some measured index variable - assumed to be proportional to local population size - exceeds an a priori threshold. We applied this principle to the spatial capture-recapture (SCR) analytical framework in a Bayesian hierarchical model incorporating capture-recapture (CR) and index information from unsampled sites to estimate density. We assessed the adaptively sampled SCR model (AS-SCR) by simulating CR data and compared performance with a standard SCR baseline (F-SCR), adaptive SCR discarding index information (AS-SCR–), and standard SCR applied at a simple random sample of sites. Under AS-SCR, we observed minimal bias and comparable variance with respect to parameter estimates provided by the standard F-SCR model and sampling implementation,

but with substantially reduced effort and significant cost saving potential. This represents the first application of adaptive sampling to SCR, and a useful framework for estimating abundance of low-density species.

Obtaining data on individual identification is often expensive to collect, and in the case of genetic identity, sometimes too sparse to perform capture-recapture analysis. We developed a methodology to estimate abundance using detection dog searches along transects for scat without the requirement of individual identity. This method estimates daily accumulation rate of scats during the survey separate from pre-existing scats, accounting for imperfect detection, and accommodates spatial covariates. Daily accumulation rate can be transformed to an estimate of population size using per-capita defecation rate. We applied the method to data collected from a moose scat survey in New York in 2016. We estimated approximately 549 (368 - 850, 95% CI) moose in the Adirondacks under the best-performing model. The method developed is an effective survey method for estimating ungulate abundance from observations of scat and does not require individual identification.

BIOGRAPHICAL SKETCH

Alec Wong was born in Queens, New York, and attended the University of Nebraska Lincoln (UNL) for a B.S. degree in Fisheries and Wildife with a minor degree in Mathematics in 2013. Since then, he has worked with The New School, The Natural Areas Conservancy of New York, and UNL on various ecological projects. He began his M.S. degree in 2015, and anticipates applying his skills in applied statistics following its completion. Alec is an avid photographer and is passionate about all things technological.

DEDICATION

It is with gratitude and humility that I dedicate this thesis:

To my advisors Angela Fuller, Andy Royle, and Jeremy Hurst first for their firm and illuminating criticism, steady pushes forward, patience, generosity, and continuing to believe in my abilities when I did not.

To Martha and Joseph Wong, my parents, whose unending support and love provided me with all the resources I needed to arrive here.

To Catherine Sun, Vanessa Springer, Benjamin Marcy Quay, Matt Paufve, D.J. McNeil, and Sarah Naiman, the best set of friends I could have during my graduate career.

To the best moose technician crew of 2016: Michael Buyaskas, Vasilissa Derugina, Carlos Fernandez, Jailene Hidalgo, Deanna Russell, and Tyler Shaban. May you all go on to achieve your dreams!

To Heidi Kretser and the staff of the WCS Adirondack Program; their support in the field, assisting with landowner coordination, logistics, local knowledge, and resources, facilitated the success of this project.

To the detection dog handlers: Suzie Marlow, Justin Broderick, Jennifer Hartman, Jake Lammi, and Mairi Poisson, whose energy, stoicism, and humor motivated all of us through the hard summer work.

Finally, to my girlfriend Lisa who offers me a fresh perspective in each conversation, and who lends me the greatest motivation in the times I need it most.

ACKNOWLEDGEMENTS

We would like to acknowledge the funding and guidance provided by the New York State Department of Environmental Conservation, Conservation Canines for their assistance in collecting the moose scat data, the U.S. Forest Service National Genomics Center for Wildlife and Fish Conservation and the Wildlife Conservation Society for assistance in landowner access and field logistics. We would also like to acknowledge Sam Peterson from SUNY ESF for assistance in field data collection.

TABLE OF CONTENTS

LIST OF FIGURES

LIST OF TABLES

Chapter 1

Adaptive sampling for spatial capture-recapture: An efficient sampling scheme for rare or patchily distributed species

Introduction

Knowledge of species abundance is a critical component of wildlife conservation and management (Williams, Nichols, and Conroy 2002), and monitoring this state variable is especially important when managing rare or endangered species. Rarity may emerge from secretive behaviors, small population sizes, or spatial clustering over large areas, such that encounters of the animal or evidence of its activity are infrequent relative to its probability of detection. Rarity poses many challenges in the estimation of abundance (W. Thompson 2013), including those related to inefficiencies in sampling. Small, highly clustered populations are difficult to sample, and may be costly when the organism of interest is absent from the majority of survey sites. Absence data are informative in analytical frameworks acknowledging imperfect detection such as capture-mark-recapture or occupancy frameworks. However, a dataset with a relatively large number of "zeroes" that arise from sampling in an area where the species is not present is costly because resources are spent gathering relatively poor information, and in addition it results in over-dispersed data that may not conform to standard statistical distributions, inhibiting inference (Barry and Welsh 2002; Martin et al. 2005). Notwithstanding an unbiased estimate, precision will be low in such situations, highlighting the importance of efficient sampling and analytical methods. Nevertheless, rare species represent an important concern for wildlife managers, usually because low population size implies a threat of extirpation or extinction, and rarity imparts a lack of critical information for management decisions.

Efficient sampling schemes for rare or patchily distributed species have been recently gaining in attention (W. Thompson 2013), but the problem has long been a focus of statistical ecology. Statistical treatments of the problem have been suggested through the use of zero-inflated Poisson or negative-binomial models (A. Welsh et al. 1996; Barry and Welsh 2002; Martin et al. 2005), wherein the abundance data are governed by a different distribution than the absence data, but others indicate that the separate modeling of absence data and abundance data implemented by the zero-inflated models has limited sensibility in terms of ecological or biological meaning (Kéry and Royle 2015). Alternatively, improvements to sampling design can attempt to address these difficulties. Stratified sampling can reduce variance in abundance estimates if the population can be partitioned by some well-defined homogeneous features; for example, if the organism is known to be strongly associated with a particular habitat type, estimator performance may be improved by allocating sampling proportionally to homogeneous habitat classes. Cluster or multistage sampling, and adaptive sampling take advantage of natural clustering of populations in order to improve inferences (S. K. Thompson 1990; Morrison et al. 2001; W. Thompson 2013).

Adaptive sampling strategies are a promising method for sampling small, clustered populations. Employing simple random sampling to estimate abundance of rare populations will result in zero-inflated data and estimators with poor precision (Salehi and Seber 1997). Often, the spatial structure of the population is not known or difficult to predict prior to surveys, making standard methods of stratification difficult to employ - adaptive sampling procedures operate only upon observed data and thus can be more effective than simple random or stratified sampling in these situations (S. K. Thompson 1990; Turk and Borkowski 2005). These methods result in preferential sampling in areas of higher animal abundance, and this framework can provide greater precision than simple random sampling among small, highly clustered populations (S. K. Thompson 1990; Salehi and Seber 1997; Brown 2003; Rapley and Welshy 2008; Smith et al. 2012). Certainly, preferential sampling – where the location of data collection is dependent upon the variable of interest – if unaccounted for can introduce bias into predictions made by the analysis. This has been examined generally by Diggle et al.

(2010) and Pati et al. (2011), and recently incorporated into the ecological literature by Conn et al. (2017). Adaptive strategies are formulated to account for non-random sampling, either by using design-unbiased estimators under strict sampling protocols (Brown et al. 2013), or by modeling the selection of data locations jointly with the variable of interest (Conn, Thorson, and Johnson 2017).

The original design-based adaptive cluster sampling (S. K. Thompson 1990) begins by implementing an initial random sample of sites to survey - termed the primary sample. A critical threshold value of the state variable of interest is selected and secondary sampling sites are generated (or "triggered") around each initial site wherever the threshold is met. Sampling resumes at each of these secondary sites, and additional sites can be triggered in turn if the threshold is met at these secondary sites. The chief advantage of this method is a distribution of effort that is a result of the spatial structure of the population. However, there exist drawbacks such as the randomness of the final sample size that make logistical constraints difficult to meet (Turk and Borkowski 2005), although there are methods that address this limitation (Christman and Lan 2001; Salehi and Seber 2002). There have been numerous contributions to variations of adaptive sampling allowing for flexible study design and inference under design-based estimators (Brown et al. 2013).

Recently, methods for studying patchily distributed populations have begun incorporating adaptive sampling principles into model-based sampling frameworks. A notable departure from the design-based adaptive sampling is the flexibility in modeling the primary sample. During the primary sample, an index variable is measured that is modeled to be conditional upon the state variable. Provided that the relationship between the index and state variables is satisfied, any valid statistical model may be used, including the ordinary case when the index variable is equivalent to the state variable. Selection of a threshold for adaptive sampling is based upon this index variable measured during the primary sampling occasion. For example, Pacifici et al. (2016; 2012) were concerned with enhancing occupancy model performance, and thus used occupancy models in the primary and secondary sampling

occasions, selecting a threshold based upon detections out of K visits exceeding some *a priori* number. Conroy et al. (2008) used occupancy models in the primary sampling occasion, also selecting the threshold based upon detections exceeding some *a priori* number, and implemented capture-mark-recapture methodology in secondary sampling for estimation of vole abundance. Pacifici et al. (2016) made additional contributions to model-based adaptive sampling methodology by incorporating a spatially-explicit occupancy model along with the adaptive procedures, demonstrating a marked improvement in confidence interval coverage, particularly when sample sizes were sufficiently large to reliably estimate spatial covariance parameters.

Adaptive sampling is especially advantageous when the sampling protocol is time consuming or expensive regardless of whether or not individuals are detected. For example, in the use of technologies such as camera trapping or noninvasive genetic sampling, establishing sampling arrays or deploying highly trained dog teams to survey sample units is extremely costly, and this cost is incurred even if a sample size of 0 is obtained. As such, it is advantageous to integrate some sort of adaptive sampling strategy in such studies.

The combination of spatial capture-recapture and adaptive sampling is motivated by an effort to estimate the current population of moose (*Alces alces*) in the Adirondacks of northern New York, an area of approximately 24,000 km^2. The moose population in this region is not growing according to management expectation, and the population was estimated at just 500-800 moose in the Adirondack park during 2010 (Wattles and DeStefano 2011). Spatial capture-recapture is an advantageous method to use for sampling moose in New York because it performs well with low-density, vagile species, and when coupled with non-invasive genetic identification of individuals from scat or hair, physically capturing individuals is unnecessary. A recent pilot study demonstrated the viability of using detection dogs to locate fecal pellets of moose in the Adirondack region (Kretser et al. 2016). A subsequent large-scale sampling effort was initiated across the Adirondacks of New York using random cluster sampling and detection of scat using trained dogs. Of 91 sites visited, 60 did not result in detection of

moose scat throughout the sampling period; this was costly with respect to time, effort, and money. The geographic rarity of moose in this system warrants the evaluation of adaptive sampling as a method to enhance cost-efficiency and sample sizes, and improve statistical certainty in parameter estimates relevant to estimating the population size of moose.

In this paper, we develop an estimator of population density for spatial capture-recapture models under an adaptive sampling scheme in which the first stage of sampling produces an index to local population size and allows more intensive sampling to be triggered based on the observed index value. We investigate the performance of an adaptively sampled spatial capture-recapture model. We validate the model's performance against a simulated population subjected to five sampling schemes, comparing the adaptive method to the ordinary SCR method when adaptive sampling is triggered by an index variable which is a function of site-specific abundance. We evaluate the performance of the adaptive sampling scheme by comparing it to an estimator based on conventional (non-adaptive) sampling based on a similar total sampling effort as well as estimators which ignore the index variable altogether. We also discuss the cost gains achieved by implementing an adaptive sampling framework and also potential application scenarios for which it might be useful.

We hypothesize that SCR implementation across all sites with index information will be unbiased with the smallest variance. Adaptively sampled SCR with index information is expected to be unbiased with greater variance than a full implementation of SCR at all sites, and the adaptively sampled SCR ignoring the index data (which results in biased sampling) is expected to be greatly biased. Under our expectations, we anticipate that the proposed method will be most useful in situations with highly patchy population distributions.

Materials and methods

Spatial capture-recapture

Spatial capture-recapture extends ordinary capture-recapture models by formally integrating spatial information inherent in animal sampling data into the probability functions describing

the detection process. Specifically, in its simplest form it makes the assumption that animal home ranges are distributed uniformly over the landscape and that detection of an individual is a function of distance from the home range centroid to the detector (Efford 2004). We describe the concepts of ordinary SCR, and then extend it to incorporate a model for the adaptive method.

Data and sampling schemes

We simulate $g \in \{1, 2, ..., G\}$ distinct populations or groups, each potentially sampled by a single transect (Figure 1.1); in so doing, referencing site or group is equivalent since the site samples one and only one population g. The transect is discretized into $j \in \{1, 2, \ldots, J\}$ segments represented by the set of coordinates $\mathbf{x}$ at which animal encounters may occur. The variable N_g denotes the group-specific population size, and the total population is $N = \sum_g^G N_g$. Any individual can belong to one and only one group, indexed for each individual by the vector $\gamma_i \in g$, having length N.

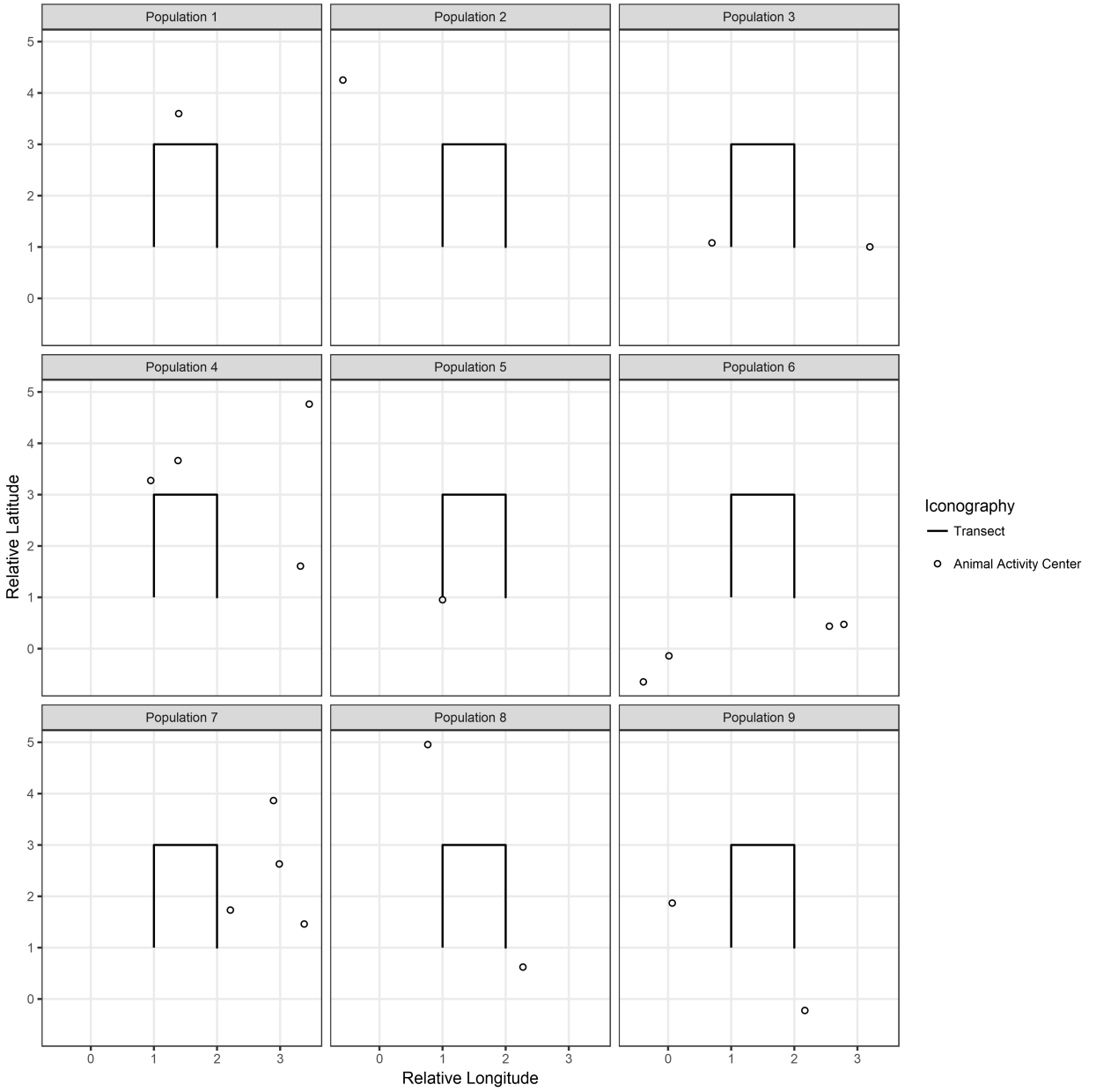

Figure 1.1: Independent animal populations are each sampled by a transect (solid line); 9 realizations of the simulation are displayed here. Animal activity centers (open circles) are distributed uniformly within the state space of each population. The population is simulated as a homogeneous Poisson point process with intensity equal to 2.

For any particular group g, let y_{ijk} denote a spatially-explicit encounter observation for individual $i \in \{1, 2, \ldots, N_g\}$ at trap or transect portion j during sampling occasion $k \in \{1, 2, ..., K\}$. Accordingly, $\mathbf{y}_g$ denotes the matrix of encounter observations for each individual

encounter at each traps within group g, also called the "encounter histories". The group-specific structure is adopted from Royle and Converse (2014) and it assumes that each group population N_g is mutually independent of one another. This is applicable in practice when trap arrays are spaced sufficiently far relative to the home range of the organism, and the sampling period is sufficiently short such that individuals do not occur in more than one group.

We propose a two-phase adaptive sampling spatial capture-recapture (AS-SCR) scheme; in the primary sampling phase, each of the G sites are sampled by some efficient method which produces an observation τ_g which we assume is an index of local population size N_g. The index could be a count obtained, for example, by road crossings of tracks of the species of interest, or counts of scat or other sign along roads or transects. The secondary phase samples a subset of size R of the G sites using a method that can produce individual animal encounters, with $R \leq G$. The selection of this subset of sites is contingent upon whether the index τ_g exceeds some prescribed threshold T: where $\tau_g > T$, the site g is sampled by capture-recapture to obtain individual animal encounters, and where $\tau_g \leq T$, only the index observations are retained; the capture-recapture sampling is not implemented.

Statistical models

SCR sites

At sites where $\tau > T$, SCR is implemented, and we estimate the population size N_{scr} as the sum of N_g among these sites,

$$N_{scr} = \sum_{g:\tau_g > T}^{R} N_g$$

incorporating standard SCR techniques into the procedure. The point process model, detection model, and encounter model are described hereafter.

Point process model

A key element of all SCR models is the introduction of a latent point process model which describes the distribution of individual home range centers or activity centers in the vicinity of the sampling array. We define $\mathcal{S}_g$ to be the two-dimensional state-space of the activity

centers $\mathbf{s}_i$ of all individuals $i \in 1, \ldots, N_g$ within group g. We assume that the distribution of all $\mathbf{s}_i$ conditional on individual group membership $\gamma_i = g$ is

$$[\mathbf{s}_i|\gamma_i = g] \sim \text{Uniform}(\mathcal{S}_g)$$

$$\gamma_i \sim \text{Categorical}(\Theta)$$

Where Θ is a vector of group-specific inclusion probabilities of length G. We use the notation $[Y|X]$ to denote the probability mass function of a random variable Y conditional on X. This formulation is consistent with a Poisson point process, which may be extended using a linear combination of covariates representing attributes of the landscape. We operate under the assumption that the state space area is constant across all g. Additionally, take $\mathbf{S}_g$ to mean the set of individual activity center coordinates for all $\gamma_i = g$.

The latent variable N_g is well-defined for any explicit specification of the state-space $\mathcal{S}_g$. Because all G populations are independent, each population has its own defined state space which is chosen to be a planar region containing each sampling array. The state space $\mathcal{S}_g$ of the latent activity center locations $\mathbf{s}$ should comprise the set of all possible coordinates that could have produced the data; however, integrating over an infinite array is not computationally practical, so the extent of the state-space is chosen large enough such that individuals with activity centers at the edge of the state space have a negligible probability of encounter, ensuring as near as possible that the expected frequency of encounter outside of the state space is 0 (J. A. Royle et al. 2014, 131–33).

Detection model

The second key element of SCR models is the specification of a model for encounter probability of an individual with activity center $\mathbf{s}_i$ near each trap or sampled unit. Most SCR models posit that the encounter probability p in a trap or transect portion j with known coordinate $\mathbf{x}_j$ is a function of distance between the individual's activity center $\mathbf{s}_i$ and the device. Sensible models for p_{ij} are monotonically decreasing whereby the value of p_{ij} decreases with increasing distance between $\mathbf{s}_i$ and $\mathbf{x}_j$. In our simulation study we use one of the most commonly used encounter probability models, based on the kernel of a Gaussian probability density function:

$$p_{ij} = p_0 \exp\left(-\frac{1}{2\sigma^2}||\mathbf{x}_j - \mathbf{s}_i||^2\right) \tag{1.1}$$

The term p_0 denotes the baseline encounter probability when $||\mathbf{x}_j - \mathbf{s}_i|| = 0$, and σ is a spatial scale parameter which relates probability of encounter of an individual in a trap to the distance between the trap j and $\mathbf{s}_i$. This model serves to describe the probability of detection, which is one part of the encounter observation model described hereafter.

Encounter observation model

Under a known-N scenario, the distribution of the encounter history data $\mathbf{y}_g$ is the product of $N_g \times J_g$ binomial probability mass functions:

$$[\mathbf{y}_1, ..., \mathbf{y}_{N_g}|\mathbf{S}_g, \sigma, p_0] \sim \prod_{i=1}^{N_g}\prod_{j=1}^{J_g} \text{Binomial}(K, p_{ij}|\mathbf{S_g})$$

where J_g represents the number of discrete transect portions within group g, and p_{ij} is as it is defined in Equation 1.1.

At the time of the survey, N_g and thus N_{scr} are unknown, so we modify the structure of the model using the method of parameter-expanded data augmentation (J. A. Royle and Dorazio 2012). A super-population M is defined where $M \gg N_{scr}$ and $M \supset N_{scr}$, and a new parameter ψ is included which describes the proportion of M that are part of the real population exposed to sampling. That is,

$$N_{scr} \sim \text{Binomial}(M, \psi)$$

$$\psi \sim \text{Uniform}(0, 1)$$

When the distribution for $[N_{scr}|\psi]$ is integrated over the prior for ψ, this is equivalent to establishing a marginal prior for the random variable N_{scr} under a Bayesian mode of inference where $N_{scr} \sim \text{Uniform}(0, M)$. The formulation with the additional parameter ψ allows a more convenient representation of the encounter observation model through a zero-inflated binomial model. Ignoring group structure temporarily, the modified observation model is as follows:

$$y_{ij} \sim \text{Binomial}(K, z_i * p_{ij})$$

$$z_i \sim \text{Bernoulli}(\psi)$$

for $i \in \{1, 2, ..., M\}$ potential individuals. If the quantity n represents the number of observed individuals, this implies that an additional $M - n$ all-zero encounter histories are added to the observation record with the goal of estimating what proportion of these $M - n$ individuals are nonexistant or "structural zeros", and which are true unobserved individuals or "sampling zeros". The term z_i denotes the inclusion index for each individual i, with $z_i = 0$ for structural zeros and $z_i = 1$ for sampling zeros. The super-population of M individuals serves as candidates to be included ($z = 1$) in the population by the MCMC algorithm.

The likelihood for the individual observations is then

$$\mathcal{L}(y_{ij}|\mathbf{s}_i, \sigma, p_0, z_i, \psi) = \binom{K}{y_{ij}} z_i \ (p_{ij}^{y_{ij}}) \ (1 - z_i p_{ij})^{(K - y_{ij})}$$

Group membership and population model

To generalize this encounter model to a stratified population with R strata or groups, we represent an individual's group membership as the variable γ_i such that $\gamma_i \sim \text{Categorical}(\Theta)$. The term Θ is a vector of all group-specific probabilities $\theta_g \in \{\theta_1, \theta_2, ..., \theta_R\}$. Definition of the vector Θ is induced by the following population model:

$$[N_1, N_2, ..., N_R|N_{scr}] \sim \text{Multinomial}(N_{scr}, \theta_1, \theta_2, ..., \theta_R)$$

where $\theta_g = \lambda_g / \sum_g \lambda_g$. This is equivalent to the Poisson model for group-specific population sizes when conditioned on the total (among all groups) population size where the Poisson mean is

$$\lambda_g = E(N_g) = \frac{N_{scr}}{R}, \tag{1.2}$$

or the expected number of individuals within any group g.

To implement the data augmentation procedure, the n observed individuals are assigned to the group in which they were observed, and the $M - n$ unobserved individuals are assigned to groups according to the group-specific probabilities in Θ, resulting in an augmented group-specific population size M_g where $M_g > N_g$. Group-specific population size N_g does not appear explicitly in the likelihood; instead it is a derived parameter obtained by summing

the values for z_i for those individuals within group g such that

$$\widehat{N_{scr}} = \sum_{g:\tau_g > T}^{R} \hat{N}_g = \sum_{g:\tau_g > T}^{R} \sum_{i}^{M_g} z_i \; I(\gamma_i = g)$$

Where I is the indicator function evaluating to 1 if $\gamma_i = g$ and 0 otherwise. We emphasize once again that the sites considered here are only those where τ exceeds the threshold T.

Index observation model

For the model of index observations, the key assumption is that τ_g must be conditional on N_g in some fashion. In general, there is no explicit linkage of the index data τ_g to N_g of the SCR state-space. However, if the sample transect is the same between the primary and secondary sample, then in fact we can regard the index count as a thinning of the total encounter frequency of the SCR study. Other situations may yield satisfactory interpretations of the index; for example if the index sample is based on a transect randomly oriented through the state-space or more practically oriented in a way without first inspecting the state-space so as to avoid favorable or unfavorable portions of the state-space.

A sensible model for the index observations where $\tau > T$ (indeed, the classical "index assumption") is consistent with the following model:

$$\begin{aligned} \tau_g &\sim \text{Poisson}(N_g * c) \\ c &= \exp(\beta_\tau) \end{aligned} \tag{1.3}$$

where c is some scalar adjustment parameter, and β_τ is the underlying coefficient to be estimated. One might interpret the index variable as a thinning of the total encounter frequency of the SCR study, and the thinning rate is thus absorbed into c. In this manner, $\hat{N}_g$ derived from the encounter observation model is used to inform the estimation of $\hat{\beta}_\tau$.

Non-SCR sites

Notably, where $\tau \leq T$ the second SCR sampling phase is not implemented, and so there are no encounter observations yielding information about N_g at those sites; a distinct model must be used to estimate N_g. The model for these sites relies on the propagation of information about N_g from the expected population size λ_g as well as from the index observations with

the following relationship:

$$\tau_g \sim \text{Poisson}(N_g * c)$$

$$N_g \sim \text{Poisson}(\lambda_g)$$

$$c = \exp(\beta_\tau)$$

$$\lambda_g = \exp(\beta_0)$$

The expected population size is indirectly informed from the encounter observation model through θ_g, which is in turn informed by the observed individual group membership γ_i. Other natural index models are possible, which we discuss later in the discussion.

For the total population size at all $G - R$ of the sub-threshold sites, we indicate:

$$N_{index} = \sum_{g:\tau \leq T}^{G-R} N_g$$

and the total number of individuals estimated at all G sites is:

$$\widehat{N_{total}} = \widehat{N_{scr}} + \widehat{N_{index}}$$

Joint distribution of the data

The joint distribution of the index data and the SCR data is represented by the following:

$$\prod_{g:\tau_g \leq T}^{G-R} [\tau_g|\lambda_g, c] \times \prod_{g:\tau_g > T}^{R} [\tau_g|N_g, c] \times [\mathbf{y}_g|\mathbf{S}_g, \sigma, p_0, z][z|\psi] \tag{1.4}$$

The distribution of the index data at the sub-threshold sites appear as the left term, and the distribution of the index data and the encounter data appear as the right term.

For sampling schemes ignoring the index observations, the terms containing τ_g are removed from the joint distribution, and what remains is the typical observation model for group-specific SCR:

$$\prod_g [\mathbf{y}_g|\mathbf{S}_g, \sigma, p_0, z][z|\psi]$$

Prior distributions

We have established one prior distribution previously – that of $[\mathbf{s}|\gamma_i = g]$, being assumed to be uniform over the state space of $\mathcal{S}_g$. Here, we establish prior distributions for the remaining variables.

The baseline detection probability parameter has prior distribution $p_0 \sim \text{Uniform}(0, 1)$ (assuming geographic coordinates are scaled to units of km).

The spatial scale parameter has prior distribution $\sigma \sim \text{Uniform}(0, 10)$.

The data augmentation parameter has prior distribution $\psi \sim \text{Uniform}(0, 1)$.

The mean group-specific population size has prior distribution $\lambda_g = \exp(\beta_0)$ and $\beta_0 \sim \text{Normal}(0, 0.01)$.

The scalar multiplier has prior distribution $c = \exp(\beta_\tau)$ and $\beta_\tau \sim \text{Normal}(0, 0.01)$.

Joint posterior distribution

The joint posterior distribution of the model parameters conditional on the observed encounter history data and index data is the product of the joint distribution for the data, and the prior distributions:

$$\prod_{g:\tau_g \leq T}^{G-R} [\tau_g|\lambda_g, c] \times \prod_{g:\tau_g > T}^{R} [\tau_g|N_g, c] \times [\mathbf{y}_g|\mathbf{S}_g, \sigma, p_0, z][z|\psi] \times \prod_{g}^{G} [\mathbf{S}_g][\sigma][p_0][\psi][c][\lambda_g]$$

For the cases where adaptive sampling is not done, so that we only have SCR encounter history data, the terms including τ are removed, leaving the posterior distribution for a basic SCR model:

$$\prod^{G} [\mathbf{y}_g|\mathbf{S}_g, \sigma, p_0, z][z|\psi] \times \prod^{G} [\mathbf{S}_g][\sigma][p_0][\psi]$$

Simulation study

Design

We evaluate the situation where $\lambda_g = 2$ for all g, specified by the relationship in Eq.(1.2). This parameterization appears reasonable to the authors for studies of animals that occur at relatively low densities. We use the threshold value $T = 4$, and we simulate the index values τ_g according to the relationship in Eq.(1.3), where N_g is the result of the simulated group population size, and $c = 3$. For each simulation we generated $G = 100$ populations sampled on $K = 3$ occasions with a single rectangular transect represented as point detectors spaced at 0.1 unit intervals along its length (Figure 1.1). A total of 1000 simulations were generated

with these parameter settings.

For added generality, the reader may use a gamma-Poisson mixture to model populations more dispersed than the Poisson scenario – the description of this model formulation can be read in Royle et al. (2012). The code used for generating the data, simulating capture histories, and analysis under the following model configurations are available for replication (Wong, Fuller, and Royle 2018).

Model configurations

Five model analyses are used to evaluate three sampling schemes (AS-SCR, F-SCR, and SRS-SCR, defined below) that either consider or ignore the index measurements obtained in the primary sampling phase (Figure 1.2). We evaluate the sampling schemes of AS-SCR considering (*AS-SCR+*) and ignoring (*AS-SCR–*) index observations, F-SCR considering (*F-SCR+*) and ignoring (*F-SCR–*) index observations, and SRS-SCR without index observations (*SRS-SCR–*).

AS-SCR+ is the proposed adaptive sampling procedure that we test for bias and precision. We expect to observe unbiased parameters estimates, particularly estimated population size.

AS-SCR– represents an preferential sampling situation and we expect it should be positively biased for density, because it samples only high-density areas without integrating information obtained from indices that fall below the index threshold.

F-SCR+ is the ideal and most costly sampling procedure, incorporating SCR and index observations at every site, and it represents the most accurate and precise baseline to which we compare *AS-SCR+*.

F-SCR– represents a standard SCR procedure implemented at all sites without the index data, which we expect will resemble *F-SCR+* with a slight loss in precision. This is an ordinary application of SCR against which we test our new procedure.

SRS-SCR– represents application of standard SCR at a simple random sample of sites equal to the corresponding number of sites sampled by AS-SCR. It makes no use of index data. This

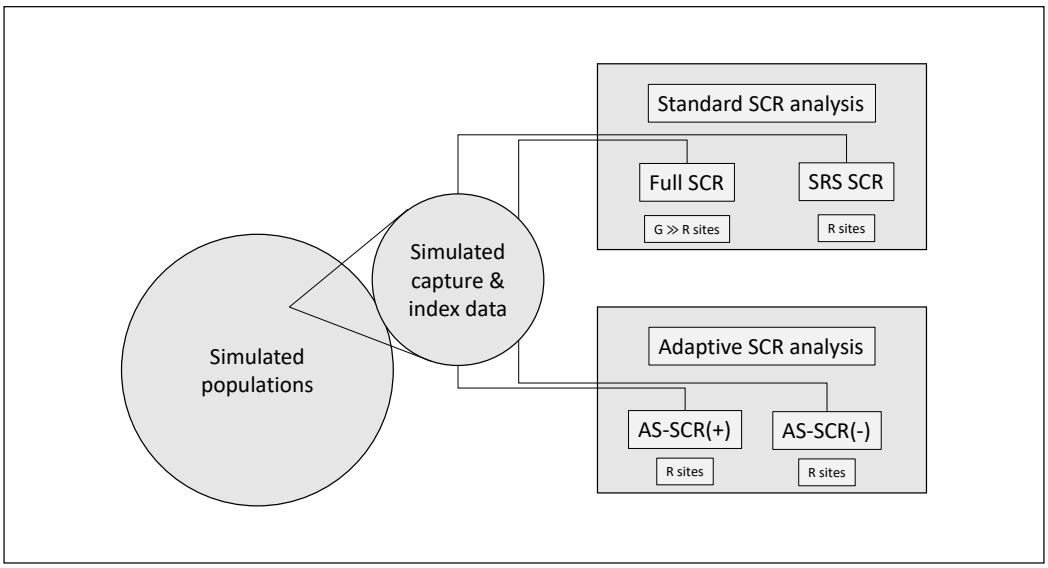

Figure 1.2: Four combinations of analytical and sampling methods are tested against simulated data. Two standard SCR analyses are performed on the full set of G sites, and also a subset of R randomly selected sites. Two adaptive SCR analyses are performed on R sites with the index exceeding a threshold τ. The plus and minus designations indicate whether index data is incorporated into the estimation procedure, or not, respectively.

comparison is important to include because it is a sampling method which a cost-restrained survey could adopt having little initial information regarding the local population. We expect this will be unbiased, but also that it will have the poorest precision in comparison to the other models in the set due to the relatively sparse information it gathers.

For each analytical procedure, we calculated relative bias, mean squared error (MSE), and 95% coverage for the parameter estimates. We transformed estimates of abundance into density to make them comparable across all models and sampling procedures. We report these summary statistics for estimates of density $\hat{D}$, scale parameter $\hat{\sigma}$, and baseline detection probability $\widehat{p_0}$, the three main parameters of interest in SCR.

Relative bias was calculated as:

$$RBIAS = \frac{\frac{1}{n}\sum_{i=1}^{n}\hat{\theta}_i - \theta_i}{\theta_i}$$

Where $\hat{\theta}_i$ is the posterior estimate for parameter θ at simulation i with true value θ_i.

MSE was calculated as:

$$MSE = \frac{1}{n}\sum_{i=1}^{n}\left(\hat{\theta}_i - \theta_i\right)^2$$

For reporting coverage, we estimated standard error using the Monte Carlo standard error estimator, used to construct Bayesian 95% credible intervals.

$$\hat{\sigma}_{mc} = \sqrt{\frac{1}{n}\sum_{i=1}^{n}\left(\hat{\theta}_i - \hat{\mu}\right)^2}$$

Where, $\hat{\mu}$ is the sample mean of all posterior estimates for parameter θ such that $\hat{\mu} = E(\theta)$, assuming the stationary distribution is achieved at all simulations.

Bayesian analysis

We evaluate these models numerically with the JAGS software implemented in R with the package "jagsUI". Ten-thousand MCMC iterations were performed for each model analysis with burn-in ranging from 500-1000 iterations. The software sampler was allowed to adapt under default settings.

Results

As anticipated, percent bias and MSE are positive and high for the preferential sampling procedure that disregards the index data (AS-SCR–), with abundance overpredicted by approximately 46% on average (Table 1.1). Additionally, coverage is very low, with the 95% credible intervals for $\hat{D}$ intersecting the true value 2.1% of the time (Table 1.2). Values of $\hat{\sigma}$ and $\hat{p_0}$ are unaffected by the omission of index information.

Table 1.1: Relative Bias for Parameter Estimates

Model	$\hat{D}$	$\hat{\sigma}$	$\hat{p_0}$
AS-SCR+	-0.0198	0.0284	0.0056
AS-SCR-	0.4586	0.0045	-0.0021
F-SCR+	0.0025	0.0091	-0.0003
F-SCR-	0.0128	0.0045	-0.0008
SRS-SCR	0.0183	0.0077	0.0023

Table 1.2: Coverage for Parameter Estimates over 95% credible interval

Model	$\hat{D}$	$\hat{\sigma}$	$\hat{p_0}$
AS-SCR+	0.8880	0.9340	0.9480
AS-SCR-	0.0210	0.9540	0.9580
F-SCR+	0.9189	0.9595	0.9505
F-SCR-	0.9560	0.9500	0.9580
SRS-SCR	0.9030	0.9570	0.9500

Table 1.3: Mean Squared Error for Parameter Estimates

Model	$\hat{D}$	$\hat{\sigma}$	$\hat{p_0}$
AS-SCR+	0.00003	0.00706	0.00014
AS-SCR-	0.00111	0.00928	0.00013
F-SCR+	0.00002	0.00482	0.00010
F-SCR-	0.00005	0.00721	0.00010
SRS-SCR	0.00011	0.01280	0.00020

Table 1.4: Posterior Standard Deviation for Parameter Estimates

Model	$\hat{D}$	$\hat{\sigma}$	$\hat{p_0}$
AS-SCR+	0.0036	0.0560	0.0083
AS-SCR-	0.0093	0.0672	0.0082
F-SCR+	0.0032	0.0491	0.0073
F-SCR-	0.0050	0.0598	0.0073
SRS-SCR	0.0068	0.0806	0.0100

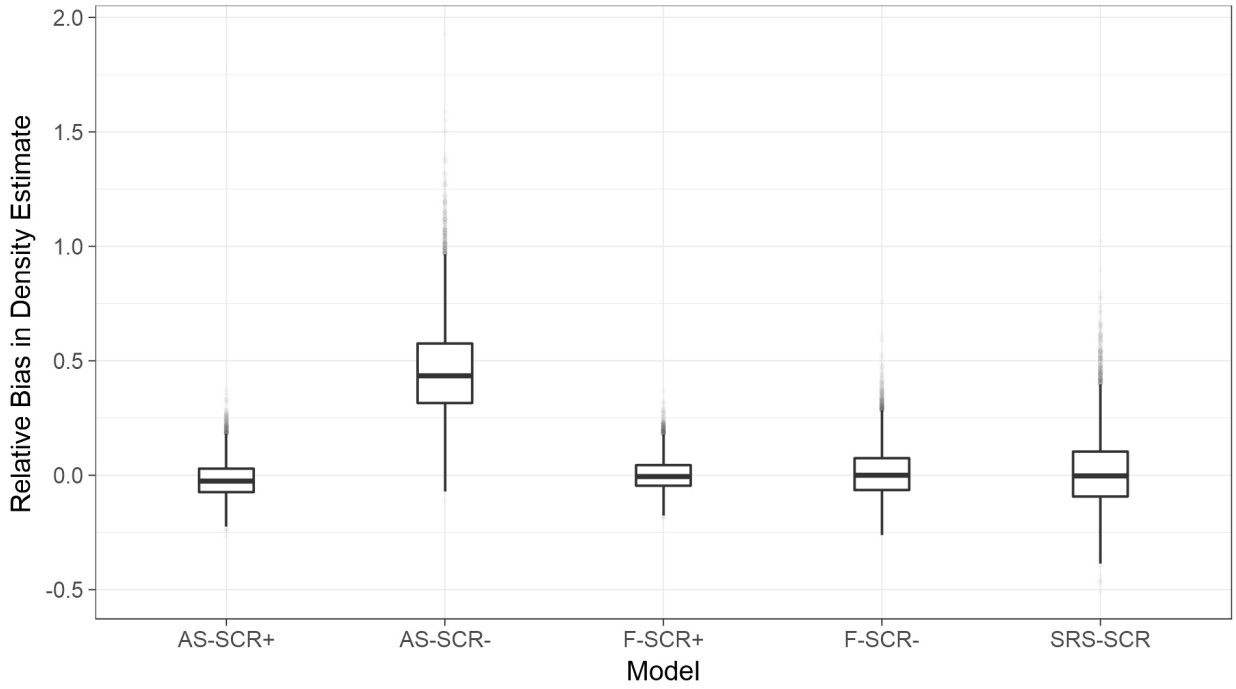

Figure 1.3: Graphical comparison of model performance. We show the distribution of relative bias in the density estimates for each model. The solid horizontal lines represent the median relative bias, the boxes represent the interquartile range, and outliers are represented by transparent dots.

In comparison, our new adaptive sampling method (AS-SCR+) has low bias and MSE (Table 1.3; Figure 1.3); bias is within 2% of the true density value, and coverage is high, with the true value included within the 95% credible interval approximately 89% of the time (Table 1.2).

The results for the baseline comparisons (F-SCR+; F-SCR–; SRS-SCR–) are unsurprising; their estimates for all parameters are unbiased and have very high coverage. Notably, the bias, MSE, and coverage for $\hat{D}$ are nearly equal between AS-SCR+ and SRS-SCR–, but the standard deviation in the estimate under AS-SCR+ is nearly half that under SRS-SCR– (Table 1.4). As F-SCR+ is the most information-rich, it is unsurprising that its bias, MSE, and estimate standard deviations are the smallest.

Under the Poisson random population simulation setting, the adaptive procedure sampled one-half of the total number of sites compared to the full treatment with virtually no loss

in estimation accuracy or precision. The AS-SCR+ estimator also estimated density with a higher precision than the equal-sized SRS-SCR application.

Discussion

Discussion overview

We present an adaptive sampling approach to spatial capture-recapture sampling that can be used to increase sample sizes for a nominal cost or reduce the cost in obtaining a target sample size, as compared to a simple-random-sample application. This application is especially relevant for low-density, patchily distributed species, which typically present significant logistical and statistical challenges.

The adaptive method distributes sampling effort in accordance to the spatial structure of the population, ideally minimizing sampling in areas of low population density. Pacifici et al. (2016) demonstrate that incorporating a spatially-explicit model for the variable of interest enhances parameter estimation, either by spatial process models or by spatial random effects (also explored by Johnson et al. (2013)). The incorporation of spatial capture-recapture with adaptive sampling may be preferable to a non-spatial model. The formulation of spatial capture-recapture in this simulation study used a homogeneous Poisson point process to represent the animal activity centers, but it could be easily extended to incorporate an inhomogeneous Poisson point process in which the assumption of uniform density is relieved, potentially allowing for more refined prediction of abundance to unsampled areas (J. A. Royle et al. 2014).

Our results suggest that adaptive SCR is equally effective as a full treatment of SCR under a Poisson randomly distributed population. While we did not perform a formal cost analysis, it is easy to consider the potential cost-savings of reducing the number of distinct sites to visit. In the motivating context, the daily cost incurred by scat detection dog surveys was approximately $1000 USD daily in 2016, whether or not moose were present on the transect. Transects with no scats composed approximately 2/3 of all the transects visited, and 91%

of these remained without scat throughout the sample period. At maximum efficiency four sites could be visited per day, making the per-site cost at least $250; with 40 unoccupied sites, the cost of allocating effort to these sites was at least $10,000, or 10% of the summer's expenditures. Under an ordinary SCR survey, equal cost and effort is spent at unoccupied sites as occupied sites, reducing efficiency when unoccupied sites compose the majority of sites visited. After implementing the adaptive SCR procedure in 2017, we observed a four-fold increase in moose fecal sample collection with no additional effort, indicating the substantial benefits in applying the method in cases where the organism of interest is sparse on the landscape.

Previous studies of design-based adaptive cluster sampling methods are known to be sensitive to the choice of adaptive threshold (Turk and Borkowski 2005; Brown 2003). The selection of the threshold value directly affects the resulting within- and between-network variances, and due diligence is required to maximize efficiency of the adaptive procedure over a simple-random-sample implementation. A similar application of adaptive sampling to model-based sampling frameworks by Conroy et al. (2008) indicates relative insensitivity of abundance estimates to a range of threshold values. However, the flexible structure of our framework precludes a general suggestion; selection of a proper index value is best informed by pilot surveys and simulation under the most applicable index model for the study system evaluated on a case-by-case basis.

The specific type of index should be carefully selected such that there is some quantifiable relationship between the index and local population density. For example, in the motivating context, the index variable was the number of scat piles encountered on the first visit to the site. Selection of a poor index measure will not bias the spatial capture-recapture parameter estimates, but sampling conditional upon this index measure – if truly uncorrelated with the population – will likely result in a sampling procedure resembling a simple random sample without an *a priori* defined number of sites visited.

Extension of results

The adaptive SCR model can accept many varieties of index model. We considered our model suitable to describe fecal deposition as a function of population size. Alternative models can vary to accommodate the study system. For instance, one may wish to formulate the model conditional on detection/non-detection of an animal:

$$x_i \sim \text{Bernoulli}(1 - (1 - r)^{N_i})$$

Where, x_i is the detection of a species at site i, r is an individual detection rate, and N_i is the local population size. One might also wish to integrate occupancy as the index model as done in Conroy et al. (2008) or Pacifici et al. (2016) and select a threshold of the occupancy estimate or raw initial count to trigger adaptive SCR.

Theoretically, the index model could also be based upon citizen science data, increasing the applicability of this model at wide spatial extents and further reducing the cost burden on researchers. For example in New York, occupancy of moose was estimated using reported observations from hunters (Crum et al. 2017), and could be augmented through the use of citizen science apps such as iSeeMammals (Sun et al. iseemammals.org) which collects presence/absence observations of mammals from hikers and camera stations. The adaptive site selection could proceed by selecting a threshold of estimated occupancy across the survey area, reducing the burden of index data collection to the researchers. The potential for sampling or detection bias in citizen science is recognized (Kéry et al. 2010), so we expect that some collection of index data would still be required from the researchers to minimize this bias, but further research in this area is warranted.

Application of AS-SCR may be particularly useful when covariates affecting density are weakly correlated or unknown, permitting efficient investigation of novel study systems since the resulting distribution of sampling effort is conditional upon observed data. Alternatively, if covariates are known that are strongly correlated with density, it may be possible to condition the index model on these, eliminating the need to conduct a preliminary index survey. This possibility also warrants further testing.

Spatial capture-recapture has been demonstrated to be more effective than non-spatial methods in estimating density of rare and elusive organisms, such as large carnivores, than non-spatial methods (Kéry et al. 2011; Sollmann et al. 2013; Blanc et al. 2013). However, data requirements for spatial capture-recapture are larger than ordinary capture-recapture methods owing to the additional parameters to estimate, so there is a larger trade-off between sampling intensity and the spatial extent that may be surveyed. This problem is exacerbated by low-density populations, where data richness is not even across the survey area. The adaptive method actively achieves focused sampling intensity at sites with greater data richness, allowing for greater potential precision than a simple random sample could typically achieve under the same circumstances. We suggest that the application of the adaptively sampled SCR method can be particularly useful when it is critical to reduce cost and effort to meet budget or time constraints while at the same time maintaining reliable parameter estimates.

Chapter 2

Quantification of moose (*Alces alces*) population from scat counts made by detection dogs

Introduction

Estimates of animal abundance are one of the most central components of conservation and management of wildlife populations (Kohn et al. 1999, Efford 2004). Methods for inferring abundance of wildlife populations must account for the fact that it is impossible to observe all individuals perfectly (Williams et al. 2002). In general, methods for estimating animal population density can be relative, using simple counts of sign or animals as an index of animal density, or explicit, leveraging understanding of uncertainty in animal detection to estimate true abundance (*i.e.* distance sampling, capture-mark-recapture, catch-per-unit-effort) (Seber and Schwarz 1999).

Human observers or passive detectors (e.g. snares, live-catch traps, camera traps) are routinely used in ecological surveys, while the use of trained detection dogs in ecological surveys is relatively recent. Use of detection dogs began only in the 1990s with increasing attention due to the high efficiency of dogs detecting target species, high accuracy in species differentiation, and obviating the need for attractants such as scent lures (Long et al. 2007). Trained detection dogs have the ability to detect odors up to 400 m under optimal conditions, and the method is independent of visual identification of scats which has been documented to confuse human researchers (Wasser et al. 2004). Detection dogs have near-perfect accuracy in locating scats of the species of concern among non-target species; Smith et al. (2003) demonstrate 100% accuracy of their trained dogs in encountering 329 kit fox (*Vulpes macrotis mutica*) scats among coyote (*Canis latrans*), striped skunk (*Mephitis mephitis*), and American badger (*Taxidea taxus*) scats. Long et al. (2007) demonstrated that detection success of trained dogs

was minimally affected by factors including wind, precipitation, temperature, topography, and openness of the site in the forests of Vermont, but these factors have been shown to affect dog scenting ability to some extent in the past (Wasser et al. 2004). Application of detection dogs in ecological surveys has also increased in part due to the advent of genetic identification of individuals from scat, enabling application of capture-recapture methodologies (Smith et al. 2003, Wasser et al. 2004, Sutherland et al. 2018).

Capture-recapture abundance estimation frameworks typically obtain information regarding imperfect detection through replicated observations of individuals, and so explicit knowledge of individual identity is central (but see Chandler and Royle (2013)). With scat surveys, identification of the individual is possible using DNA left on the surface of the scat from the epithelial lining of the lower intestine. However, individual identity is not always attainable or affordable, and methods for analysis of pellet survey data are available to estimate abundance in the absence of individual identity.

Distance sampling is routinely used for abundance estimation in the context of pellet surveys, which accounts for detection error through application of protocols to induce structured variation in detection probability that can be modeled explicitly (Buckland et al. 1993, Marques et al. 2001). Usually, distance sampling is performed by human observers making observations along a transect, assuming that detection decreases with distance away from the center line. In contrast, detection dog searches are to some extent guided by the dog handler, enabling focused searches of specific areas or directed searches along a transect, but each dog and handler combination has a unique searching pattern that is not easily restricted by protocol. In addition, unlike human visual detection, detection of a target (*e.g.* scat of a particular species) by a dog is rarely a binary event with an associated 'distance of detection' upon acquisition of the target; detection dogs instead gain information slowly over time regarding the presence and location of a target, subject to wind patterns and scent within the environment, culminating in confirmation of the target once it navigates close enough and signals the handler. This process is not readily modeled in a distance sampling framework.

Additionally, it is important to account for bias induced by observation of scats that were not deposited during the survey. This can be accomplished by modeling scat decay rate, or by clearing plots or transects of pre-existing scats before sampling. Jenkins and Manly (2008) provide a method that clears portions of transects in order to model surplus scats not belonging to the time frame of the survey. However, it can be difficult or impossible to clear scats at a broad scale, and modeling decay rate involves tracking marked scats through time, which may be intractable with very slow decay rates or high spatial variation in decay rates.

In this paper, we develop a method that estimates population size by quantifying initial scat deposition separately from daily accumulation rates of scat during the survey, allowing for the relatively unstructured search patterns of detection dogs when accounting for imperfect detection. We apply the method to a survey of moose in New York during 2016. Detection dogs searched for moose scat along transects under a spatial capture-recapture methodology. Lack of amplification prevented us from using capture-recapture methods to estimate abundance, requiring the development of new methodology for estimation of population size from scat sampled by dogs.

Model development

Let $s \in 1, 2, ..., S$ be an index representing unique transects traversed by dogs. We overlay upon each transect a grid with cells of dimension 50m x 50m, enveloping all recorded dog GPS track points, and index all of the unique grid cells traversed by the dogs at any time by $g \in 1, 2, ..., G$. A grid cell is considered 'visited' if there is at least one GPS track point within the cell. Note that g is not indexed by s in any explicit manner, as g represents an identifier rather than a site-referenced index.

The dogs sample sites on primary sample occasions, indexed by $v_s \in 1, 2, ..., V_s$. There were no more than 4 total visits to any given site in 2016 (*i.e.* $\arg\max(V_s)_1^S = 4$). On an occasion v, in each grid cell g, the dogs make a known number of replicate observations $r_g \in 1, 2, ..., R_g$. The number of observations $r_g > 1$ when the dog doubles back on its path to enter a grid cell

more than once during the same occasion v. For simplicity, we refer to $\arg\max(V_s)_1^S$ as V_{max} and $\arg\max(R_s)_1^S$ as R_{max}. This structure resembles the robust design *sensu* Pollock (1991), in which marked animals are surveyed on primary sample occasions informing population dynamics parameters, as well as secondary sample occasions within the primary ones to inform detection probability (Figure 2.1).

Let λ_g be the expectation of the initial deposition of scat $\Delta_{g,0}$ in any particular grid cell before the first visit to site s. For the purpose of our analysis, we take the initial deposition as having occurred instantaneously on June 1, 2016, which is the date at which the first transect was visited that year. We model the abundance of initial deposition as:

$$\begin{aligned} \Delta_{g,0} &\sim \text{Poisson}(\lambda_g) \\ \lambda_g &= \exp(\boldsymbol{\beta} * \mathbf{X}) \end{aligned} \tag{2.1}$$

where, $\boldsymbol{\beta}$ represents a vector of regression coefficients, and X is the design matrix of an intercept and potential covariates.

Let θ_g be the daily rate of scat pile deposition per grid cell between visits to each site. The total accumulation in the interim between sample occasions is modeled as a Poisson random variable:

$$\begin{aligned} \Delta_{g,t} &\sim \text{Poisson}(\theta_g * d_{g,t}) \\ \theta_g &= \exp(\boldsymbol{\beta_\theta} * \mathbf{X}_\theta) \end{aligned} \tag{2.2}$$

where $d_{g,t}$ is days during interim t for cell g *between* visit v and $v+1$, where $v = t$. That is to say, if $v = t = 1$, then the occasion referenced by $v = 1$ is the initial deposition period, $d_{g,1}$ represents the days between the initial deposition ($v = 1$) and the first visit to site s ($v = 2$), and thus additional accumulation $\Delta_{g,1} = \theta_g * d_{g,1}$ depends upon the length of time between $v = 1$ and $v = 2$. In this way, the dimension of $d_{g,t}$ is $G \times (V_{max} - 1)$.

If a grid cell has only one visit for the duration of the survey, then the vector $d_{g,t}$ consists of the days between June 1 and the first visit to the site represented in $d_{g,1}$, and 0's proceeding for

all $1 < t < V_{max} - 1$. In this way, we constrain accumulation to be 0 after our last observation, because modeling these values is of no consequence to estimation of the parameters since there is no information about scat quantity after the final visit. Note that $d_{g,t}$ is identical for all cells g that belong to a particular site s, whether or not the cell was visited on a particular visit v, since we are modeling accumulation of scat independent of our activity.

Let $y_{g,v,r}$ be the count of scat collected within any particular grid cell g on occasion v and replicate r. Note that $y_{g,v,r} = 0$ in two scenarios - when the grid cell was visited and no scat are found, or when the grid cell was not visited. We model the observations of counts of scat (and separate these two interpretations of $y = 0$) as independent Binomial trials:

$$\begin{aligned} y_{g,v,r} &\sim \text{Binomial}(N_{g,v,r},\ p_{g,v,r}) \\ p_{g,v,r} &= p_0 * \text{vis}_{g,v,r} \end{aligned} \tag{2.3}$$

In the simplest case, we treat the probability of detection as homogeneous across all g, v, and r. If covariates on detection were desired, a logit link would be applied to p;

$$p_{g,v,r} = \frac{\exp(\boldsymbol{\beta_p} * \mathbf{X}_p)}{\exp(\boldsymbol{\beta_p} * \mathbf{X}_p) + 1} * \text{vis}_{g,v,r} \tag{2.4}$$

In the above equations for p, we multiply p by $\text{vis}_{g,v,r}$, an array of dimension $G \times V_{max} \times R_{max}$. This array is filled with binary indicators for visitation of a particular grid cell g on sample visit v, in the r^{th} replicate, with $\text{vis}_{g,v,r} = 1$ having made a visit, and $\text{vis}_{g,v,r} = 0$ having not – call this array the visit array.

This visit array is important in that it constrains the probability of detecting scat to be 0 when there was no dog track within a grid cell g in a particular visit to site s on occasion v. If the site was visited fewer than 4 times (*i.e.* $v_{max} < V_{max}$), the visit array constrains detection probability to be 0 on visits $v > v_{max}$. This allows us to maintain consistent dimensions for the matrices for $\mathbf{y}$, $\mathbf{d}$, $\boldsymbol{\Delta}$, $\mathbf{p}$, and $\mathbf{N}$, which is convenient for computational reasons (see below).

The number of successes $N_{g,v,r}$ in the Binomial trial in Equation 2.3 represents the quantity of scat in cell g on sample occasion v in replicate r available to be observed. It is modeled as deterministically dependent upon removals $\mathbf{y}$, and stochastically dependent upon the accumulation $\mathbf{\Delta}$ in the following relationship:

$$\begin{aligned} N_{g,v,r}|_{v=1} &= \Delta_{g,0} \\ N_{g,v,r}|_{v>1,r=1} &= N_{g,v-1,R_{max}} - y_{g,v-1,R_{max}} + \Delta_{g,v-1} \\ N_{g,v,r}|_{v>1,r>1} &= N_{g,v,r-1} - y_{g,v,r-1} \end{aligned} \tag{2.5}$$

During $v = 1$, $N_{g,1,r}$ is the realization of $\Delta_{g,0}$ according to Equation 2.1, for all r, because there were no removals during this initial deposition period. During the first visit to a grid cell g in occasion $v = 2$, $N_{g,2,1}$ is the initial abundance minus the collections made in the initial deposition period (which is always 0), plus the daily accumulation that was generated according to Equation 2.2. If there is any replication of observation of grid cell g (*i.e.* $r > 1$), then $N_{g,v,r}$ is whatever was available in the previous replicate $r - 1$ less any collections made during that replicate. The mechanism of this model for the available scat N omits possible degradation of the scats, which we assume to be negligible over the course of the survey (91 days).

Estimation of the per-cell daily deposition rate θ_g is the central component by which we make inference regarding density of moose. We obtain information about θ_g from sites with repeated visits, but also from those with just a single visit due to the inclusion of elapsed time since June 1. The temporal lag between the first visit to a site and the first visit to another site later in the season provides additional accumulation, in theory, that should be evident in the expectation of collections made from those sites. We do not use an estimate of the total abundance of scat piles over the course of the survey to estimate moose density because we cannot assume knowledge of the deposition period and degradation rate of scats leading up to the initial deposition, which is necessary to infer the number of individuals using the areas.

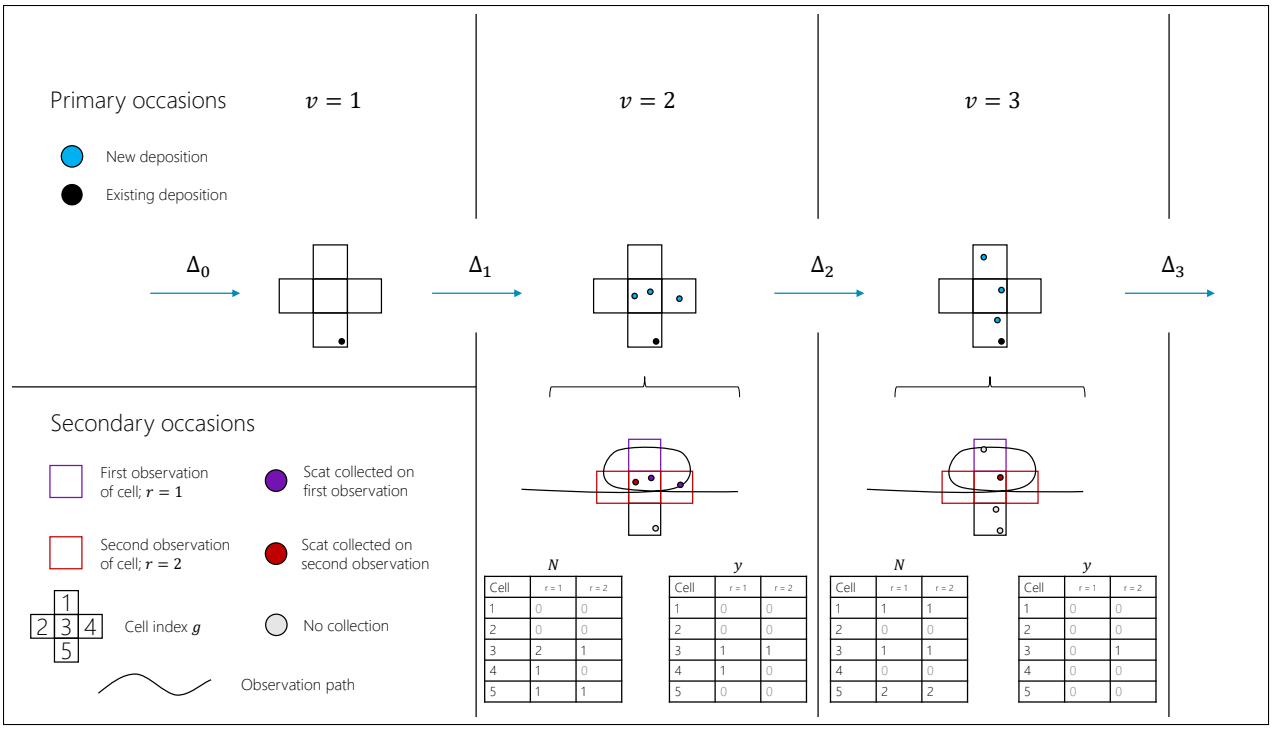

Figure 2.1: Displayed is the mechanism for the latent population model, and observations across visits v and replicates r, in the context of five grid cells.

Having obtained an estimate $\hat{\theta}_g$, an estimator for moose density is:

$$\hat{D}_g = \frac{\hat{\theta}_g}{A_g * \delta} \tag{2.6}$$

where, δ represents daily *per-capita* defecation rate, and A_g is the area of a single grid cell. The value for δ was drawn from literature sources observing captive and free-ranging moose (Miquelle 1983, Joyal and Richard 1986, MacCracken and Ballenberge 1987). Because δ is unknown to us apart from values in the literature, we used a parametric bootstrap to incorporate the uncertainty regarding the population per-capita daily defecation rate, fitting the sample means described in the literature to a gamma distribution to obtain a distribution of δ. This estimator is advantageous in that the estimate for moose density applies only to the period within the confines of the survey, from June 1 to the last visit of the last site s, and it is be modeled independently of the state of the population leading up to the survey that left the initial deposition $\Delta_{g,0}$.

We used a Bayesian estimation framework. The joint distribution of the data is:

$$\prod_{g}^{G}\prod_{v}^{V_g}\prod_{r}^{R_g}[y_{g,v,r}|p_{g,v,r},N_{g,v,r}][N_{g,v,r}|\Delta_{g,0},\Delta_{g,t}][\Delta_{g,0}|\lambda_g][\Delta_{g,t}|\theta_{g,t}]$$

according to the equations developed previously, and thus the posterior distribution is proportional to:

$$\prod_{g}^{G}\prod_{v}^{V_g}\prod_{r}^{R_g}[y_{g,v,r}|p_{g,v,r},N_{g,v,r}][N_{g,v,r}|\Delta_{g,0},\Delta_{g,t}][\Delta_{g,0}|\lambda_g][\Delta_{g,t}|\theta_{g,t}]\times[\lambda_g][\theta_g][p_0] \tag{2.7}$$

We used uninfomative prior distributions for the parameters. For p_0 we used $p_0 \sim \text{Uniform}(0,1)$. For the expected initial deposition rate λ_g and daily deposition rate θ_g we used $\lambda_g, \theta_g \sim \exp(\text{Uniform}(-20,5))$. We used the normal prior $\text{Normal}(\mu = 0, \sigma = 100)$ for all regression coefficients.

We analyzed the model using JAGS (Plummer 2017) called from R (R Core Team 2017). JAGS was allowed to adapt for ten-thousand iterations, and then the `autojags` function was implemented to proceed *ad infinitum* until convergence was deemed sufficient, or as long as possible. In all models there were an excess of 68,000 samples from the posterior distribution.

Application

In the Adirondack Park of New York State, surveys were performed using detection dogs between June 1 and August 31, 2016. We employed the detection dog training company Conservation Canines who supplied five dogs and three handlers. The dog breeds were a mix of Australian cattle dogs, Labrador retrievers, and other mixed breeds, and they were trained using scats collected from Adirondack moose.

Dogs searched 3 km triangular transects, discarding all scat encountered on the first visit, and collecting samples on all subsequent visits. Dogs searched off-leash, guided by the accompanying handler following the flagged transect line. Eighty-seven transects were visited in 2016, which were arranged by random cluster sampling (see Appendix A for details of transect siting). Primary cluster centers were distributed randomly across the Adirondacks,

and two sub-cluster centers were generated approximately 10 km apart from each other. Each sub-cluster was composed of three transects separated by approximately 4 km apart on average, and no closer than 1 km. It was ensured that each transect was accessible by road such that each cluster could be sampled in a day, for the purpose of efficiency. This design was intended to maximize the variation in distance between observations of individuals, to optimize inference into spatial capture-recapture parameters. The GPS location of each scat encounter was recorded, as well as the GPS locations of the dogs' movements at roughly 1 second intervals. A total of 872 scats were encountered.

Upon parameters λ and θ, we applied spatially continuous covariates including UTM northing, elevation, highway density, and minor road density (see Appendix B for details on covariates). We also modeled categorical effects of habitat, with categories of coniferous, deciduous, mixed, and wetland habitats. The covariates were resampled on a grid with a resolution of 1000 meters. We predict that moose density will be positively related to northing and elevation, and negatively related to highway and minor road density. We make no hypotheses regarding the relative direction of the categorical habitat covariates (Appendix B).

For detection probability p, we assessed the effect of track length within a searched grid cell, assuming that detection would increase with increasing length of the track within the cell. This may be important to account for, because a grid cell is considered to be fully observed given the inclusion of a single GPS point within it (see Figure 2.1); this assumption is made more reasonable by including the length of the track in the grid cell as a covariate.

All continuous covariates were scaled and centered for this analysis, and were masked by a polygon layer approximately 1700 km^2 expected to have no moose occurrence (i.e. open water or hamlets/large human settlements, as defined by the Adirondack Park Agency Land Classification dataset).

We used the estimator for moose density given by Eqn. 2.6, evaluating θ_g at each grid cell according to the relationship specified in Eqn. 2.2. While it is theoretically possible to assess combinations of these covariates on λ and θ separately, the number of coefficients to be

estimated drastically increased the time of analysis to an impractical point. It was decided that λ and θ would share the covariate coefficients to minimize the parameters estimated; this is reasonable because it was observed that the scat count during the initial visit was highly indicative of subsequent collections, so it follows that initial deposition λ should reflect similar relationships with the covariates as the subsequent daily accumulation rate θ.

We evaluated the models under four covariate configurations:

1. Null Model: The null model without any covariate effects
2. Distance covariate model: A model with only the track distance covariate on the detection parameter p.
3. Human deterrence model: A model with northing, elevation, highway density, and road density on process parameters, and track distance covariate on the detection parameter.
4. Habitat model: A model with northing, elevation, and habitat on process parameters, and track distance covariate on the detection parameter

Results

The process and observation parameters had some difficulty converging (assessed using Gelman-Rubin (G-R) statistic and G-R diagnostic plot) in most models, attaining G-R statistic values of ≤ 1.3. However, across large variation in starting values, the parameter estimates reliably returned to consistent point estimates. Agreement between the models regarding moose abundance provided additional confidence that the samples were drawn from the true posterior, albeit with autocorrelation in the sample draws, reducing effective sample size of the MCMC posterior samples. In contrast, the continuous covariate coefficients converged quickly with Gelman-Rubin statistics equal to 1.0 in all models including them. Figures 2.2 and 2.3 illustrate the parameter estimates with credible intervals, and the direction of covariate relationships with deposition rate θ in the case of the covariate coefficients in Figure 2.3.

Our sampling was not representative of the full population distribution of elevation (Appendix

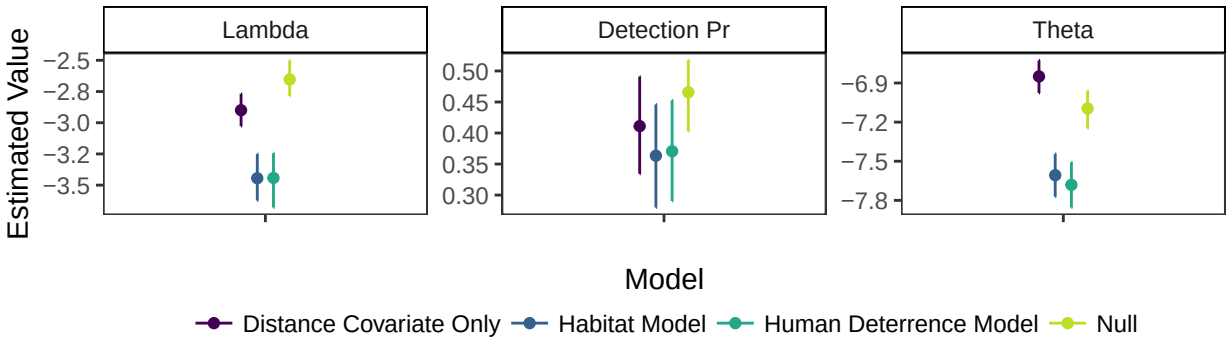

Figure 2.2: Process & observation parameter estimates. The bars shown are 95% credible intervals.

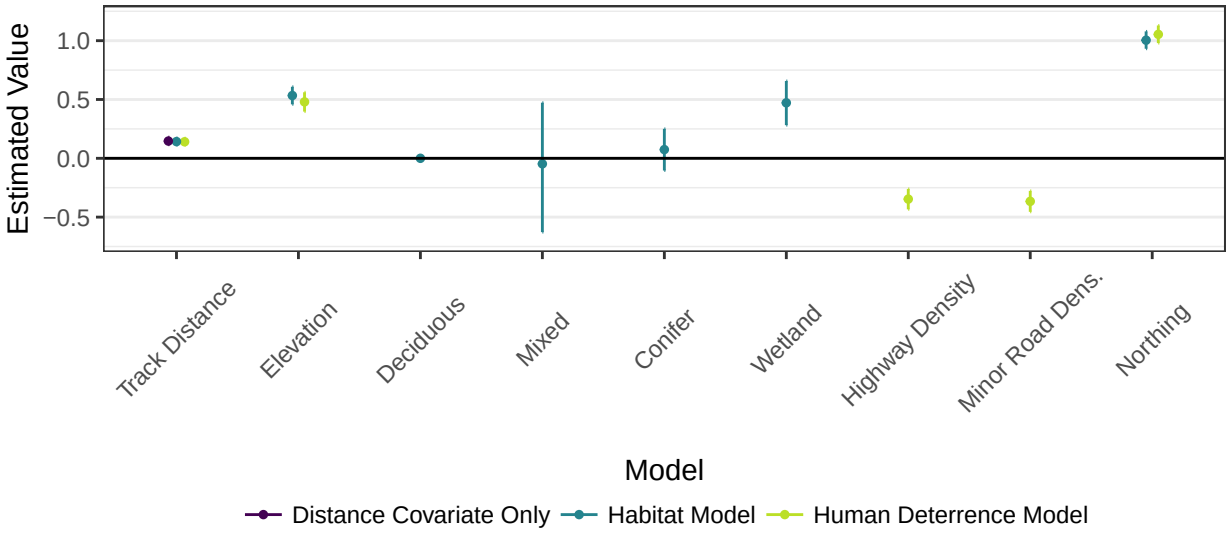

Figure 2.3: Coefficient estimates for spatial covariates. The bars shown indicated 95% credible intervals. Deciduous has been fixed to 0 to serve as the reference category to which the effects of Mixed, Conifer, and Wetland are compared.

C), and so the elevation values in the High Peaks montane region of the park likely does not reflect the same relationship with moose density as measured in our sampling. Therefore, we performed the prediction omitting values above the top 99% of elevation, acknowledging the insufficient representation of elevation within our model. Prediction across the full elevational gradient and other methods of prediction are discussed in Appendix C.

Estimates of moose density are provided in Table 2.1 for each of the models and treatments of elevation. The confidence limits are derived from application of the upper and lower bounds of the 95% credible interval of the estimate for θ in predicting abundance. The bootstrapped upper and lower bounds are derived from evaluating the 2.5% and 97.5% quantiles of the bootstrapped defecation rate applied with the 95% credible limits for theta, respectively, to calculate moose abundance, through Equation 2.6.

Table 2.1: Estimation of moose abundance within the Adirondack Park, sampled with detection dogs between June 1 and August 31, 2016. The null model contains no covariate effects on process or detection parameters. The distance model contains an effect of track length within a grid cell on detection parameter p. The human model contains landscape effects of northing, elevation, highway density, and minor road density on process paramters, and track length on the detection parameter. The habitat model contains landscape effects of northing, elevation, and habitat (categorical) on process paramters, and track length on the detection parameter.

Model	Mean	Lower CI	Upper CI	Lower CI bootstrap	Upper CI bootstrap	DIC
Null Model	549	471	629	368	850	9874
Distance Model	701	618	793	480	1074	98728
Human model	740	593	964	431	1412	75833
Habitat model	631	425	979	309	1435	323783

Discussion

We developed a method to estimate abundance from index observations that does not rely on individual identity. This method can replace capture-recapture surveys, saving the time and

cost of marking animals or performing genetic analyses. The method is also less restrictive in protocol than distance sampling, enabling surveys of large transects on the order of kilometers, and the use of detection dogs to increase rate of detection.

Ordinarily, several sources of bias inhibit estimation of abundance from scat; it is important to correct for bias from the detection process, and from scats within the survey area that existed prior to the survey. Correction of the second source of bias has seen relatively little attention, but it is key to estimating abundance; if unaccounted for, the period of observation is effectively unknown because one cannot always distinguish between fresh scats deposited during the survey and those that may have been pre-existing. Assuming that the period of observation is that of the survey results in an overestimate of abundance.

A solution is to clear plots entirely upon the first visit, but this is an impossibility at large scales, such as that of our survey. Another method is to model the decay process in order to estimate the period to which observations of scat belong, but this requires marking fecal groups and following their decay process and becomes intractable with greater spatial complexity and time to decay (Laing et al. 2003, Jenkins and Manly 2008). Jenkins and Manly (2008) use paired transect segments that were cleared or not cleared to estimate and account for the surplus observations due to uncleared plots. Our method is similar to this method, except our model eliminates the need to clear any plots, instead modeling the pre-existing scats and new accumulations directly, allowing for the simplest survey protocol of the options described here.

We applied the methodology to a study of moose in the Adirondacks of New York. The best model, assessed by deviance information criterion (DIC), was the null model, followed by the human deterrence model; however, the difference in DIC indicates that all other models do not fit the data as well as the null model. For the purposes of estimating moose population size, we use the results of the null model, and estimate that there are approximately 549 moose (95% CI: [368, 850]) in the Adirondack Park.

All of the model estimates of moose density are reasonable given previous information

regarding the abundance of moose in New York (but see Appendix C). A concurrent study examining moose population size using aerial surveys by the State University of New York College of Environmental Science and Forestry has estimated comparable predictions of abundance with a mean of approximately 394.14 moose (95% confidence limit: [297.7, 521.79]) (Frair (2017) *personal communication*). The difference in the estimates may be due to poor sightability of moose within dense conifer regions with the aerial survey method, as we observed slight or equal relative effect of conifer to the more easily observed deciduous habitat. Previously, informal conjectures of abundance from moose sighting and moose-vehicle collision data have given no indication that the population has exceeded 1,000 individuals between 2008 and 2010 (Hickey 2008).

Our model assumes that there is no degradation of scats, violation of which would result in an underestimate of moose abundance. While we consider the period of the survey (3 months) short enough to meet this assumption, this model could possibly be extended to accommodate decay of scats in the fashion of open population models such as the Jolly-Seber model (Jolly 1965). If θ represents 'recruitment' of scats, then let ψ represent the 'survival' probability of scats. This new paramter ψ would allow modeling of degradation rate should this be sufficiently high, eliminating potential bias from the assumption of no decay.

The detection process may depend on features of the scat, such as freshness, pile size, morphology (pelleted versus amorphous), etc. Since we model detection at the level of the grid cell, modeling covariates of individual scats is not possible within this framework. Reformulating the model to accommodate covariates on the level of the scat would require re-casting the observation process as Bernoulli trials assuming simultaneous observation of all scats upon visitation of a grid cell. Each scat would have observation histories that are all 0 until it is detected, as well as an explicit model to track the entrance of scat piles into the population, perhaps using a data augmentation procedure to estimate the number of scats that went unobserved over the course of the survey, similar to the method described by Gardner et al. (2010) and Royle and Dorazio (2012).

Another assumption that our model makes is the Poisson distribution for both initial deposition of scats, as well as daily accumulation. It may be more reasonable in our model to employ a negative binomial representation for the distribution of scat deposition to model extra-Poisson variation, which may be necessary due to the preponderance of empty grid cells. One may also attempt to reformulate this into a spatially-explicit model using an inhomogeneous point process, or model intensity dependent upon a Gaussian random field in a log-Gaussian Cox process. This would require implementation in optimized techniques such as INLA (Rue et al. 2009) or NIMBLE (de Valpine et al. 2017).

We developed this method *post-hoc*, but the method could be improved through protocol. Identification of process parameter values relies on being able to determine the rate of detection, and this is best measured through repeated sampling of areas, as we described in the development of the model. Deliberate and random replication of observation would provide a more robust estimate of detection probability, since we cannot verify that grid cells replicated in the 2016 survey were done so independent of scat presence. Linear transects could be walked twice, once to the end and back, offering replication at all grid cells visited, providing increased quality of data for estimating p. The model would likely benefit from less clustering of the transects, which was a result of designing for spatial capture-recapture. Our method is tailored to the use of detection dogs, and should be implemented with them for two reasons. First, the assumption of full observation of a grid cell upon entering it is more reasonable with dogs than humans, and second, the rate of detection with human observers is likely to be far lower than the 30-50% we estimated with detection dogs.

The method described herein may serve as an effective survey method for ungulates. Unlike aerial surveys, most environments are able to be sampled efficiently, and in multiple seasons, but a cost analysis would need to be performed to identify the optimal pattern of employment of aerial or dog surveys to monitor moose populations in the future. Nevertheless, this method represents a method to obtain estimates of population size that is simple and flexible in survey protocol, analysis, and interpretation of results.

APPENDICES

A. Initial methodology for estimation of moose population size: spatial capture-recapture and genetic identification via microsatellite analysis of scat

Spatial capture-recapture (SCR) is an advantageous method to use for sampling moose in New York because it performs well with low-density, vagile species (Kéry et al. 2011, Blanc et al. 2013, Sollmann et al. 2013), and when coupled with non-invasive genetic identification of individuals from scat, physically capturing individuals is unnecessary (Wasser et al. 1997). This framework is not only useful for eliciting population size, but also studying patterns in animal resource selection, landscape connectivity, and movement (Royle et al. 2018), offering a potentially rich source of information for addressing management concerns.

Capture-recapture methods account for bias in detection of individual animals through repeated observations of individuals in distinct temporal occasions, assuming that the animal is equally detectable in each occasion, or that variation in detection can be modeled using covariates. Spatial capture recapture methodology models additional variation in detection that is a function of distance between the point of observation and the animal's home range center, an unobserved variable. Detections at multiple distances are therefore important to estimate parameters of space use (σ) within the context of SCR, as well as repeat observations of individuals (Royle et al. 2014).

A pilot study performed by Kretser et al. (2016) in 2008 demonstrated the viability of using detection dogs to locate fecal pellets of moose in the Adirondack region. Following this result, in 2016 the authors contracted Conservation Canines to perform sampling for moose scat,

determining that sampling two transects of approximately 3 km in length per day per dog unit would be a practical upper limit. Given the time frame of the survey – from June 1 to August 31, 2016 – an upper limit of 91 transects could be visited over three sampling occasions. An additional clearing visit was to be made to each site to eliminate pre-existing scats to the best of the dogs' ability.

An optimal survey design for an SCR study will provide ample data containing multiple observations of individuals, with high spatial variance in detections. Ideal arrangements of SCR survey units are clustered (Sun et al. 2014), and so we opted for a clustered random survey design. The cluster spacing was determined by simulating animal activity centers and transect survey data under varying spacing from 0 km to 10km, using a value of σ (a parameter of space use) derived from moose GPS collar data collected in previous years by the New York State Department of Environmnental Conservation (NYSDEC) and the State University of New York School of Environmental Science and Forestry (SUNY ESF). This separation distance was determined to be between 2000 - 4000m (Figure 3.1).

The Adirondack Park was gridded into 15 primary units to provide even sampling of the park. (Figure 3.2). Site selection proceeded by stratified random cluster sampling; primary clusters were composed of sub-clusters of three transects separated by approximately 10 km. This was for efficiency reasons, such that the clusters could be sampled completely within three days. The transects within each sub-cluster was separated by 2-4 km, according to the results of the simulation study (Figure 3.3).

The transects were flagged by technicians with flagging tape prior to the arrival of the detection dog units. A total of 68 sites were surveyed with repeat visits in the 2016 survey. Figure 3.4 illustrates the final arrangement of transects. Conservation Canines supplied five dogs and three handlers for the project. The dog breeds were a mix of Australian cattle dogs, labradors, and other mixed breeds, and they were trained using scats collected from Adirondack moose. Upon arrival to the Adirondacks, the dogs received reinforcement training in areas known to the researchers to have a relatively high density of moose. Samples of scat

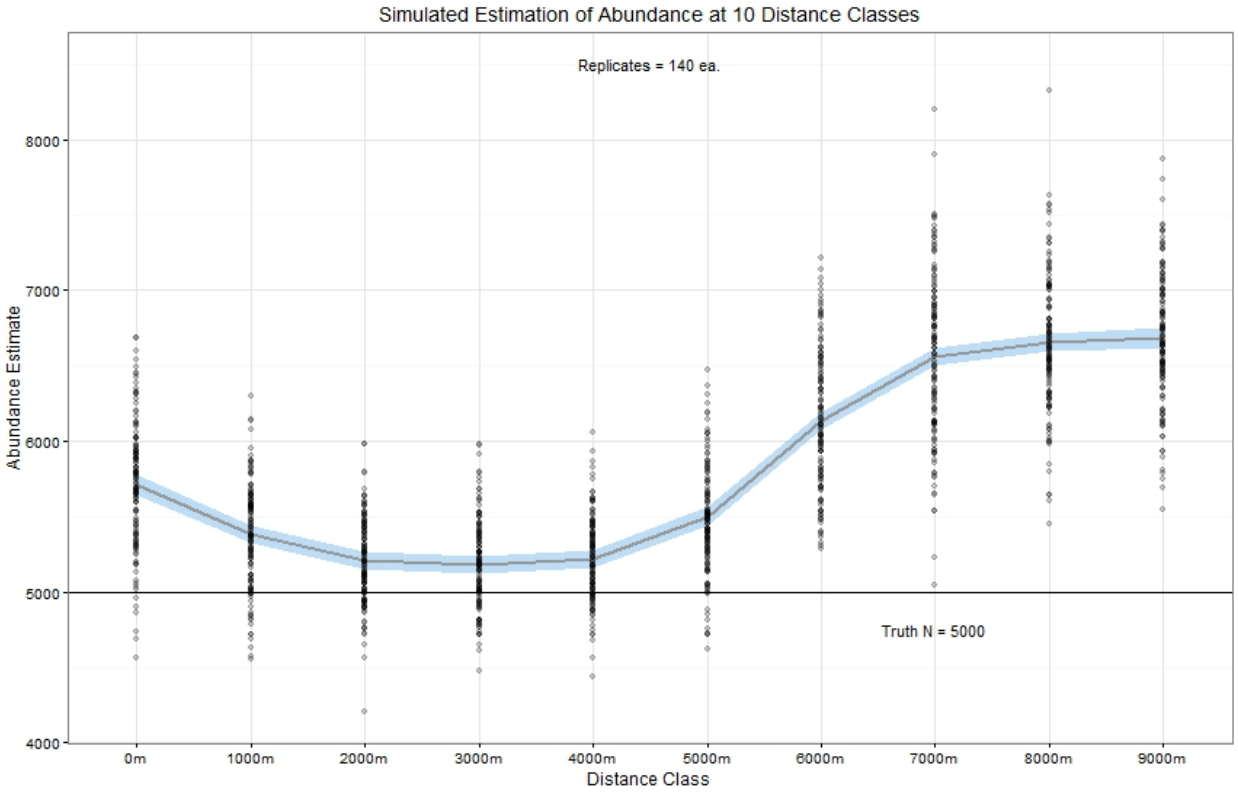

Figure 3.1: Simulation results identifying optimal minimum separation distance of transects. Bias in estimation of population size is lowest at approximately 2000 - 4000 meters of separation.

Figure 3.2: The Adirondack Park was divided into 15 primary units, in which primary clusters were sited.

were preserved by drying the pellets in paper bags using a food dehydrator. At the end of the survey, a total of 872 scat piles were encountered, and samples were taken from 236 after the initial clearing visit, which were sent to the United States Forest Service National Genomics Center for Wildlife and Fish Conservation at the Rocky Mountain Research Station (RMRS; Missoula, MT) for genetic analysis.

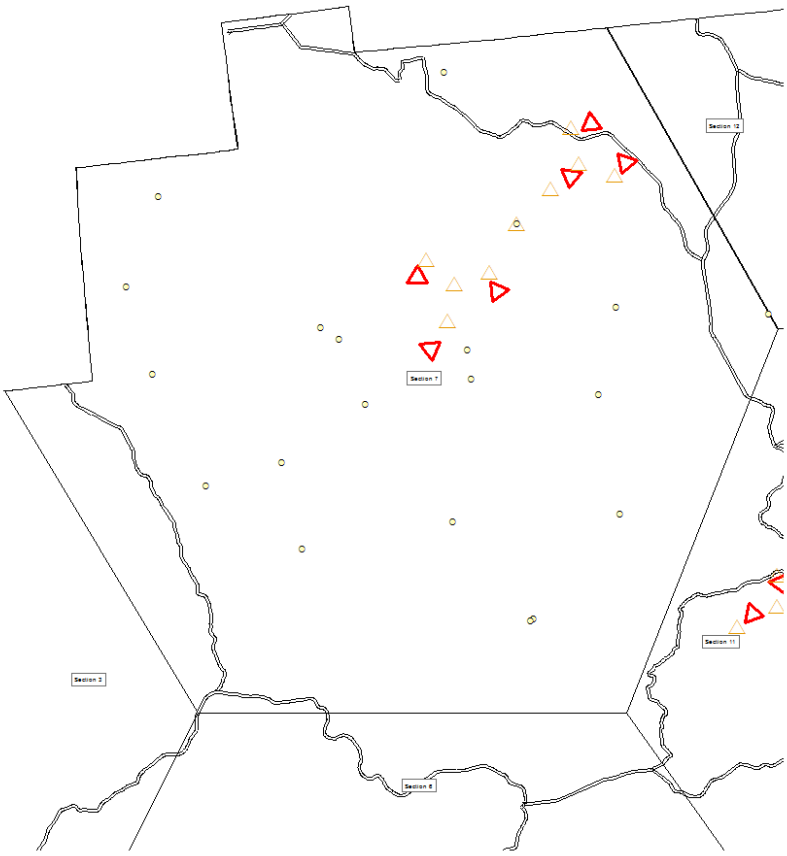

Figure 3.3: Site selection methodology for surveying moose in the Adirondacks, New York. Transects were triangular in shape and 3 km in length, placed in sub-clusters of 3. Primary clusters were composed of two sub-clusters separated by approximately 10 km. Yellow dots represent randomly selected candidate primary cluster centers. Sub-clusters were sited about the primary cluster center with random angles of rotation (orange triangles), and moved slightly to optimize access (red triangles).

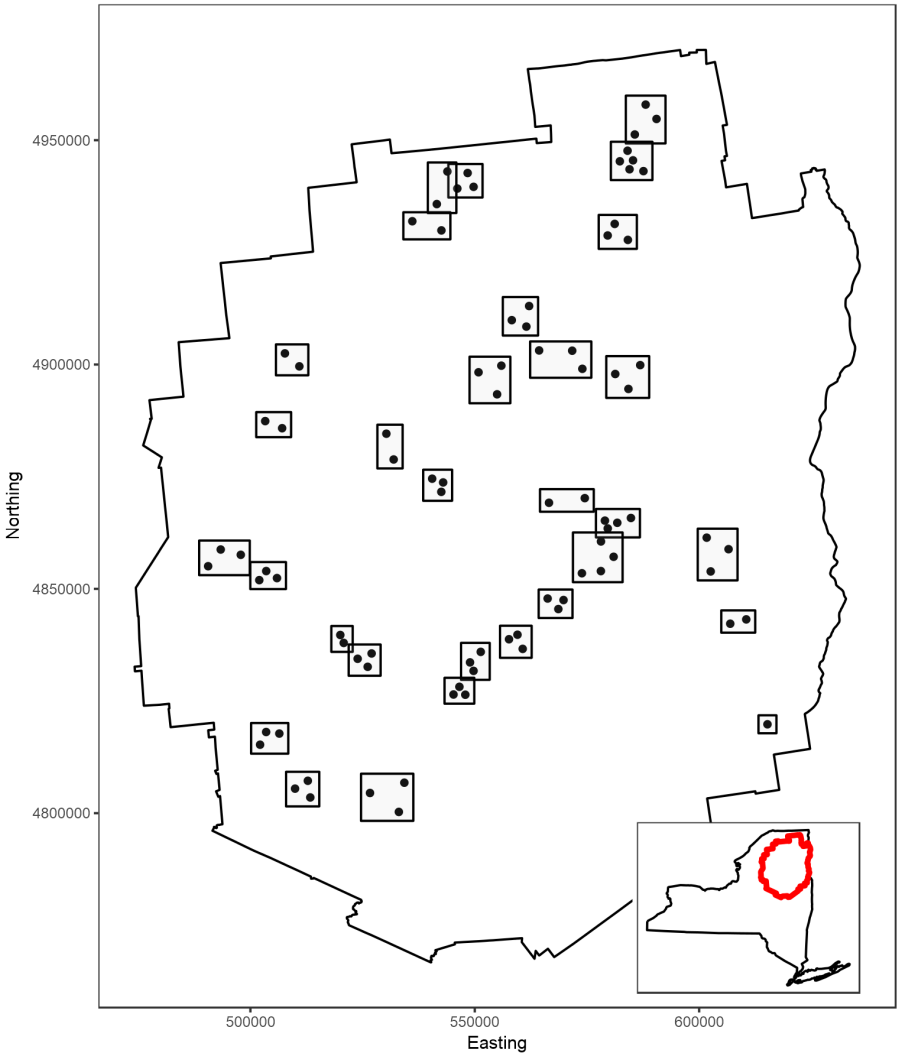

Figure 3.4: Transect locations within the Adirondack Park. Each dot represents the location of one transect, and each sub-cluster is bounded by a box. The inlaid plot indicates the extent of the Adirondack Park relative to the state of New York.

The use of noninvasive genetics in capture-recapture studies is effective because individuals can be identified from polymorphic variable number of tandem repeats, typically microsatellites (Palsboll 1999). Common microsatellites used in moose genetics have been described (Bishop et al. 1994, Wilson et al. 1997, 2015). The RMRS used panels for the following microsatellite loci for analysis of the scat samples sent to them: RT5, RT9, RT24, RT30, BM203, BM2830, BM888, BM1225, BL42, FCB193, MAP2C, T156 and T193.

The DNA was extracted using surface swabs from each pellet in each sample, according to the procedure by Brinkman et al. (2010). The extracted DNA was then amplified using polymerase chain reaction; ultimately, only 8% of the samples ($n = 21$) amplified DNA and provided a successful genotype. In contrast, the microsatellite panels provided complete genotypes for 10 tissue and hair samples collected from radio-collared moose in the Adirondacks in 2016, indicating proper functioning of the microsatellite panels. Four additional methods were attempted in order to genotype the scat samples. Phire Hot Start II DNA Polymerase (ThermoFisher Scientific) was tested on the samples using universal mammalian primers (amplifying the nuclear SOX21 gene), yielding no amplification among the samples tested. Second, an inhibitor removing tablet was used in place of an inhibitor-removing buffer, yielding no genotypes. Third, DNA was extracted instead using fine scraping of the fecal pellet exterior instead of cotton swabs, yielding no genotyping success. Finally, a PCR inhibitor removal kit (Zymo Research) was applied to 21 of the DNA extractions from swabs. These included DNA extracts from swabs that had amplified alleles at 1-5 loci (but did not amplify well enough to obtain a usable genotype, $n = 12$). No genotypes were obtained.

The spatial capture-recapture methodology was applied again in a survey in 2017, implementing a few key changes to the sampling, storage, and handling of scat samples. The period of sampling was reduced from approximately 20 days between visits to a given site to 11 days, reducing environmental degradation of DNA on the scats. The scats were frozen and shipped to the RMRS frozen with dry ice. In addition to the fecal pellets themselves, DNA extraction using cotton swabs was performed *in situ*, as well as in a laboratory setting by the field technicians. The results from the 2017 survey yielded no genotypes among a subset of 20 samples. See Appendix E for additional information regarding the 2017 field season.

Amplification of DNA under PCR reaction – particularly for scat – is sometimes subject to low success rates due to inhibitors in the sample (Rådström et al. 2004), environmental effects (Brinkman et al. 2010), temporal effects due to diet (Murphy et al. 2003, Maudet et al.

2004), among other factors requiring careful preparation of the samples (Wasser et al. 1997). Our unprecedentedly low genotyping results are hypothesized to be an effect of summer diet (*i.e.* plant secondary compounds inhibiting the PCR reaction), as PCR amplification was observed to be higher in late-winter samples (94%, $n = 16$, *unpublished*), and lower in late-spring samples (40%, $n = 10$, *unpublished*). In addition, the survey by Kretser et al. (2016) obtained an amplification rate of $\approx 28\%$ amplification success with samples collected during late spring. The lack of amplification prevented us from using capture-recapture methods to estimate abundance, prompting development of the new methodology described in the main article.

B. Commentary on covariate data and hypotheses

Roads have been demonstrated to be a deterrent to moose (Dussault et al. 2007, Laurian et al. 2012, Bartzke et al. 2015), therfore we expected to observe decreasing moose density with increasing road density. Road density was separated into highways and minor roads because they represent distinct processes; highway density represents a mortality threat to moose, whereas minor road density represents a proxy for human activity, both of which may deter moose. The road kernel density estimates were calculated under default settings in ArcMap using the tool "Kernel Density Estimate". The road data were obtained from the 2017 TIGER line dataset (Bureau 2017). The roads were divided into their respective categories because they represent different landscape processes; highways represent a mortality threat, and minor roads reflect human settlement sprawl.

Moose are adapted to cold climates and are thermally stressed in summertime temperatures exceeding 14°C (Renecker and Hudson 1986). Moose regulate their temperature by selecting shaded microhabitat to avoid solar radiation (McCann 2013) and by selecting macrohabitat types sheltered by dense conifer cover (van Beest et al. 2012, Melin et al. 2014). Additionally, temperature decreases with increasing elevation due to environmental lapse (Geiger et al. 1995), thus our hypotheses hold that moose abundance should be positively associated with northing and elevation. In the Adirondacks, the range of elevation is approximately 30m to

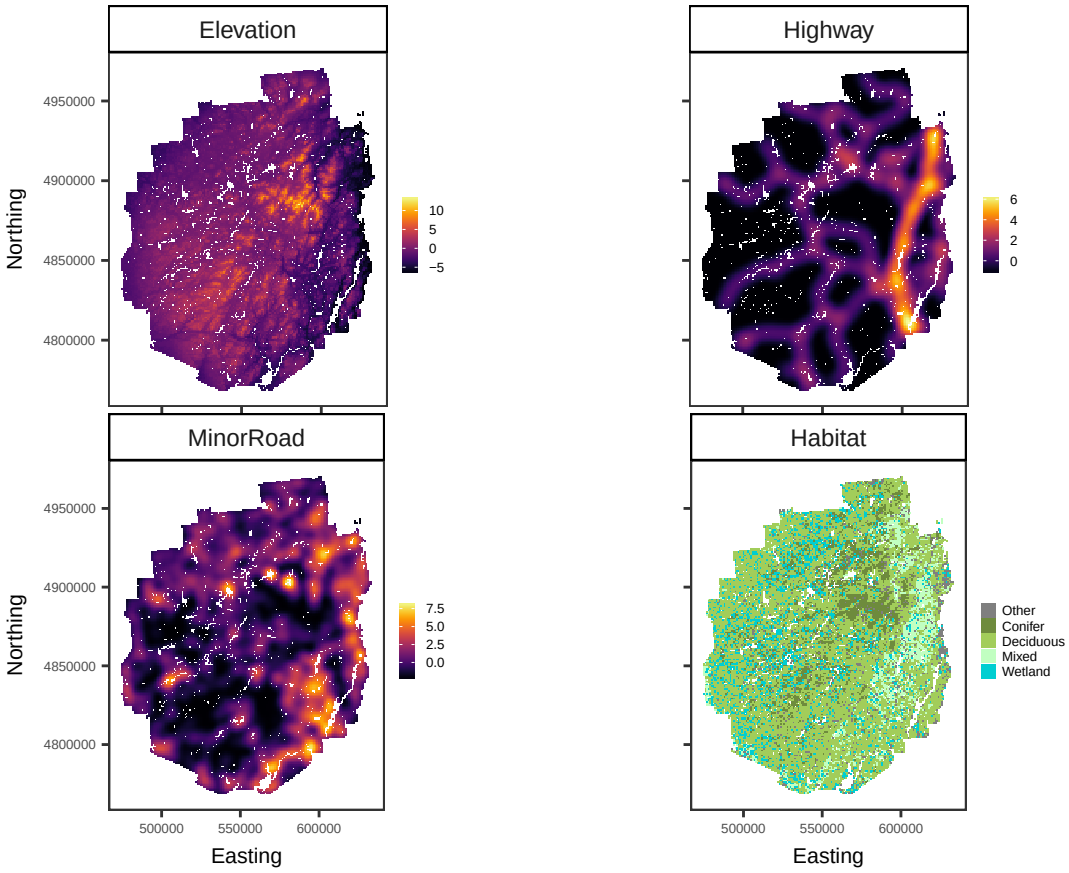

Figure 3.5: Selected covariates within the Adirondack Park, New York. The covariates were resampled from their original resolution to cells of 1000 m^2. The empty areas within the park represent the areas removed from prediction, where moose are expected not to occur, an area of 1700 km^2.

approximately 1600m, with a shift to boreal habitats at higher elevations (Figure 3.6). The elevation data was obtained from the National Elevation Dataset (Survey 2017). Easting as a covariate was not assessed in order to reduce the parameter space, and particularly because there was no hypothesized relationship between moose density and easting to our knowledge.

The relationship between habitat composition and moose is complex, with several factors affecting selection of habitat. Deciduous trees, particularly regenerating stands, provide the most nutritional forage for moose during the growing season, but moose may obtain approximately a quarter of their forage from aquatic vegetation during the summer months (Peek et al. 1976, Timmermann and McNicol 1988, Street et al. 2015); in contrast, conifer forests offer relatively poor forage quality in summer months. Yet, dense conifer cover and wetland features are important features in managing thermal stress, so we deemed inclusion of habitat variables important, but do not make any hypotheses regarding the relative direction of particular coefficients as compared to other habitat categories. Habitat was derived from The Nature Conservancy's Terrestrial Habitat Map of the northeastern U.S.A. and Atlantic Canada (Feree and Anderson 2013), and reclassified into the four categories described above. Within the Adirondacks, conifer composes approximately 10% conifer cover, 56% deciduous cover, 8% mixed forest cover, 14% wetland cover, and 12% hamlet, open water, and other incidental categories that were not included as categorical covariate levels due to their low composition of $< 1\%$ of Adirondack habitats.

The spatial distribution of abundance provided by the model with continuous spatial covariates (Figure 3.7) identifies the areas known to local researchers anecdotally to have relatively high densities of moose; for example, the Lyon Mountain area to the north, the Moose River Plains area slightly west of center, and West Canada Lakes Wilderness area just south of the center of the park. Despite having only literature information regarding per-capita daily defecation rate, the full confidence limits among all of the values (excepting the full-range elevation predictions) extends from approximately 300 moose to 1435 moose. Accounting for the additional uncertainty surrounding individual defecation rate, we can state that at the

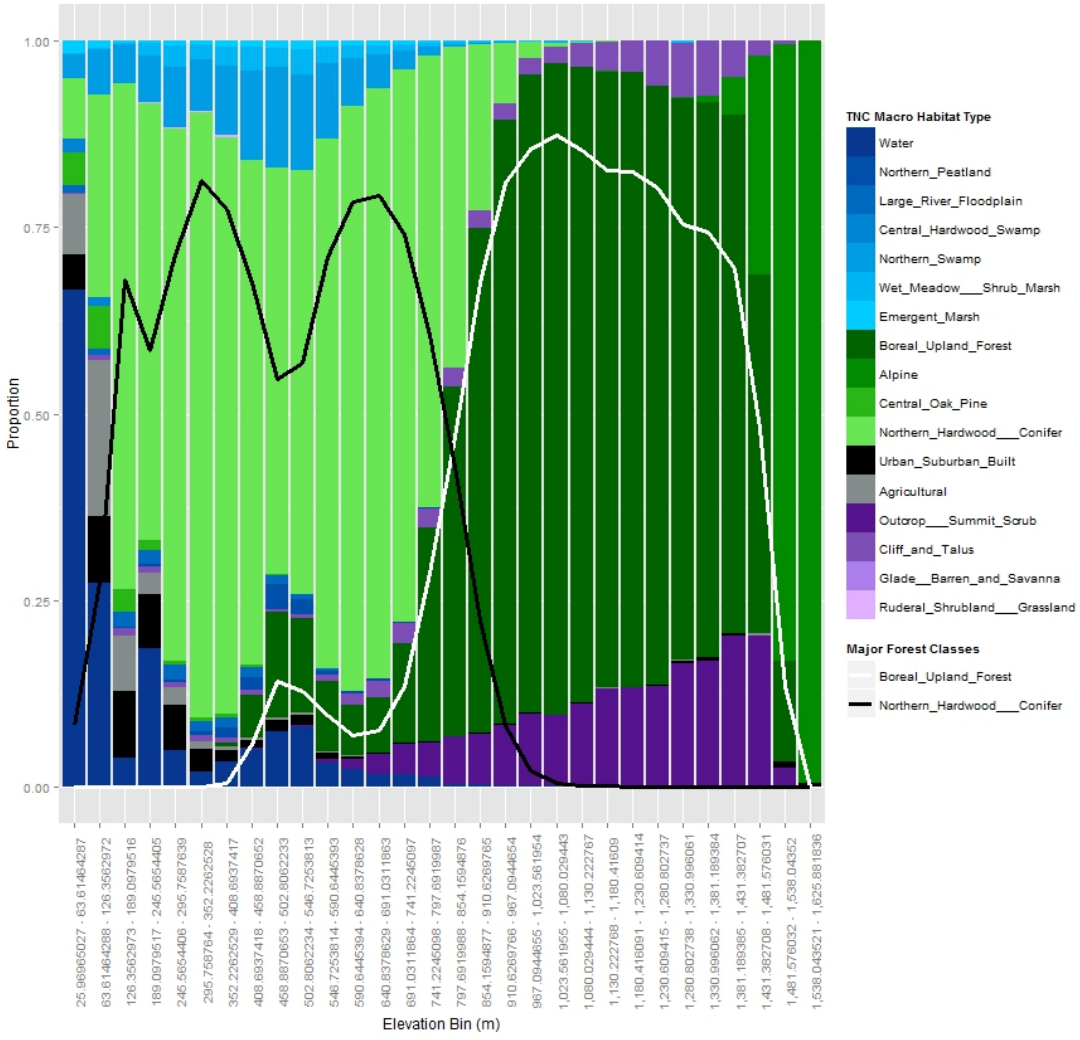

Figure 3.6: Displayed are the habitat macrogroups of the Adirondacks along the elevational axis, as defined by The Nature Conservancy Terrestrial Habitat Map. The transition between boreal forest and deciduous forest begins at approximately 800m in elevation.

very least that the population of moose has *not* increased significantly above its appraisal in recent years.

The direction of the regression coefficients aligned with our hypothesis predictions, observing a positive relationship of moose density with northing and elevation, and a negative relationship with highway and minor road density. The habitat coefficient estimates suggest that there is largely no effect of forest type relative to deciduous forest, apart from the insignificantly positive effect of conifer cover. This suggests that there is no apparent difference in the time moose spend between hardwood, softwood, and mixed forest, such that the expected rate of scat accumulation between them is approximately equal. In contrast, wetland habitat was predicted to have a positive effect on moose density greater than the deciduous category, supporting existing knowledge regarding the importance of wetland availability to moose habitat quality.

The covariate relationships with moose density suggest that thermal refuge plays a key role in the distribution of moose in the Adirondacks. Increasing northing and elevation provide reduced temperatures for a species already at the southern extent of its range, and a greater selection of wetland habitat and conifer habitat with respect to deciduous habitat may indicate moose respond to elevated summer temperatures by seeking out these habitats, potentially at the cost of optimal foraging habitat.

C. Limitations of sampling across the elevational gradient

As shown in Figure 3.8, the sampling distribution of elevation does not cover the range of the population distribution. We perform prediction of moose abundance in three scenarios:

1. A prediction at all elevations.
2. A prediction omitting values above the top 99% of elevation, acknowledging the insufficient representation of elevation within our model.
3. A prediction imputing a mean elevation above the top 99% of elevation, making the

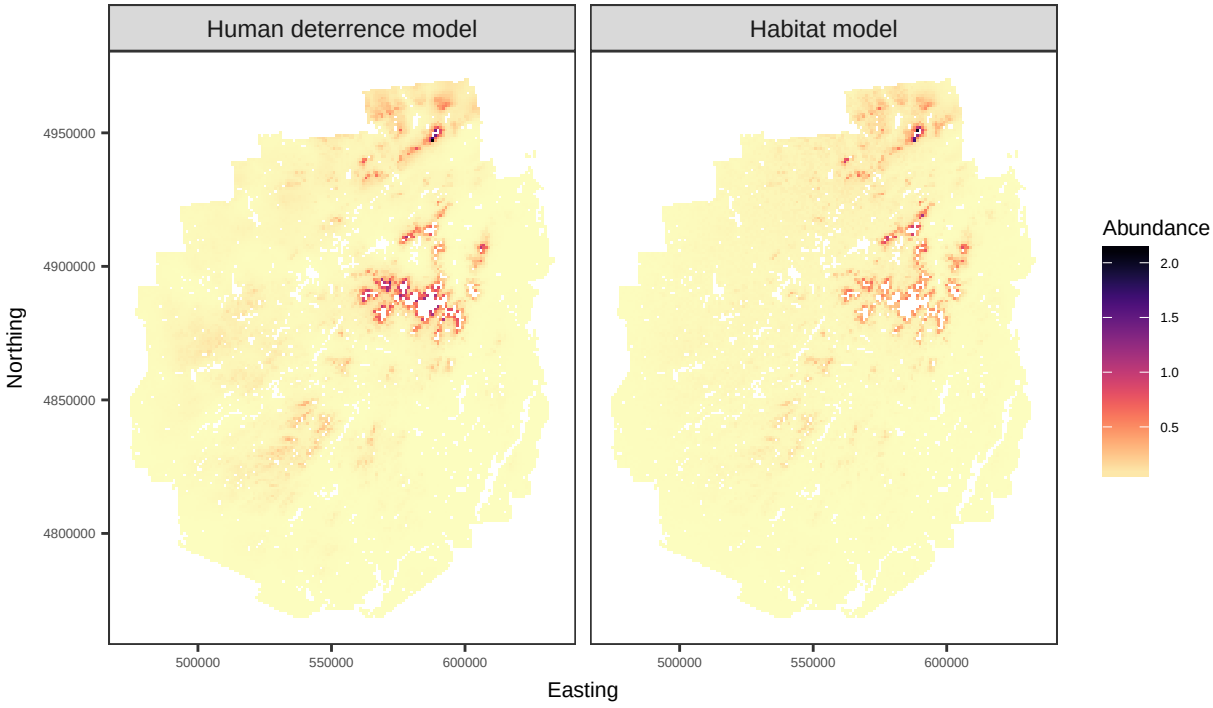

Figure 3.7: Spatial distribution of abundance of moose, using the Human deterrence model and the Habitat model, removing the 0.99%-ile of elevation. Given the area of the grid cells, the cell values also represent density per 1000 m^2.

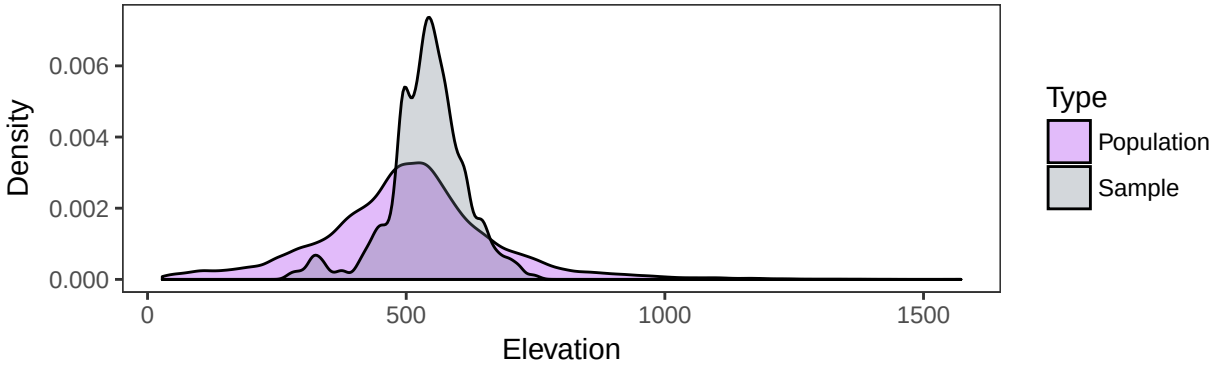

Figure 3.8: Sampled distribution of elevation versus the distribution of elevation within the Adirondacks. Elevations above 800m were unsampled, and thus not represented in our dataset.

assumption that it is an average amount and not representing the estimated relationship between elevation and density.

Figure 3.9 illustrates the elevation covariate under these three contexts described. In all three cases, 99% of the predictions are identical, and the difference exists in the remaining 1% of the grid cells at the highest elevations; above 996.78 meters in this case. All of the other covariates were sampled in proportion to their population values.

Table 3.1 contains the prediction for each scenario. There is only a trivial difference between omission of high-elevation regions and imputation of the mean elevation value. However, the estimates obtained from prediction across the full range of elevation values is suspect because it implies there are 674 moose at high elevations, an area that is 222 km^2 and composing just 1% of the park. We believe that the estimates simply reflect the lack of data above 800m in elevation. Thus we give more weight to the predictions across the trimmed elevation range that do not consider the highest values because the area is small enough to ignore and the alpine habitat at those elevations is not likely to be of high quality to moose.

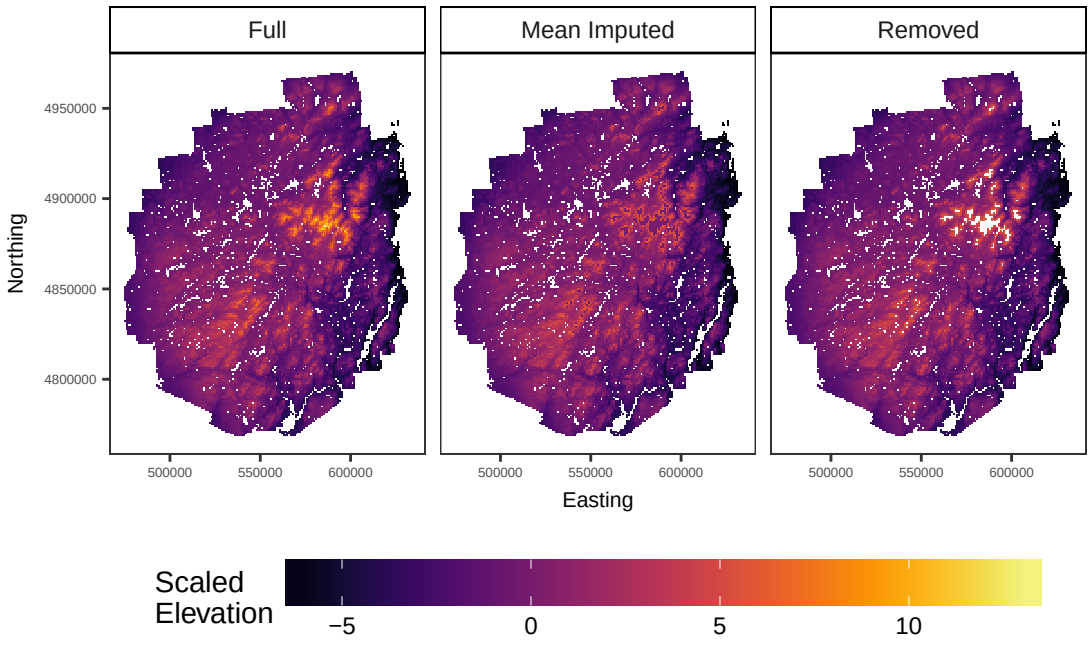

Figure 3.9: Elevations at high values were either retained, removed, or imputed with the mean elevation value for the purpose of acknowledging the limitations of the sample data in predicting beyond its range.

Table 3.1: Estimation of moose abundance within the Adirondack Park, including calculation over the full elevation gradient, and with the mean imputed above the 99%-ile.

Model	Mean	Lower CI	Upper CI	Lower CI (bootstrap)	Upper CI (bootstrap)	DIC
Null : Full Elevation	554	475	635	372	858	9874
Null : Trimmed Elevation	549	471	629	368	850	9874
Distance : Full Elevation	708	624	801	486	1088	98728
Distance : Trimmed Elevation	701	618	793	480	1074	98728
Human model : Full Elevation	1414	930	2337	675	3433	75833
Human model : Trimmed Elevation	740	593	964	431	1412	75833
Human model : Imputed Elevation	752	605	975	439	1427	75833
Habitat model : Full Elevation	1086	589	2257	428	3316	361841
Habitat model : Trimmed Elevation	631	425	979	309	1435	361841
Habitat model : Imputed Elevation	639	429	996	311	1462	361841

D. JAGS model code

The code displayed below is for the full model, having shared regression coefficients between λ and θ. All other models can be obtained from this by eliminating unwanted covariates from the code. Note that all of the levels of the categorical habitat covariate are included, opting instead to constrain the category of 'deciduous' to be the reference category, instead of eliminating it from the code.

```
# Priors
p00 ~ dunif(0,1)
pInt = log(p00/(1-p00)) # Intercept for p on logit scale
theta00 ~ dunif(-20,5) #prior for theta intercept
lambda0 ~ dunif(-20,5) #prior for lambda intercept

# Priors for landscape fixed effects
beta_hab_softwood       ~ dnorm(0,0.01) # prior for habitat effect
beta_hab_hardwood       = 0 # prior for habitat effect, made to be reference
beta_hab_wetland        ~ dnorm(0,0.01) # prior for habitat effect
beta_hab_mixed          ~ dnorm(0,0.01) # prior for habitat effect
beta_elev               ~ dnorm(0,0.01) # prior for elevation effect
beta_highway            ~ dnorm(0,0.01) # prior for highway effect
beta_minor_road         ~ dnorm(0,0.01) # prior for an index of human effect, local road density
beta_northing           ~ dnorm(0,0.01) # prior for northing effect
beta_easting            ~ dnorm(0,0.01) # prior for easting effect

# Priors for detection fixed effects

beta_detect_dist            ~ dnorm(0,0.01) # prior for distance effect

for(i in 1:nSites){

    # Model for deposition
```

```
# Initial deposition.
N1[i] ~ dpois(lambda[i])

# Linear model for lambda.
lambda[i] = exp(lambda0             *   gridCovariates[i,1]  +
                beta_northing       *   gridCovariates[i,2]  +
                beta_easting        *   gridCovariates[i,3]  +
                beta_elev           *   gridCovariates[i,4]  +
                beta_highway        *   gridCovariates[i,5]  +
                beta_minor_road     *   gridCovariates[i,6]  +
                beta_hab_softwood   *   gridCovariates[i,7]  +
                beta_hab_hardwood   *   gridCovariates[i,8]  +
                beta_hab_mixed      *   gridCovariates[i,9]  +
                beta_hab_wetland    *   gridCovariates[i,10]
                )

# Initial deposition of scats.
for(v in 1:maxV){
    N[i,1,v] = N1[i]
}

# Deposition between time 0 and first visit is found in days[i,1]
for(t in 1:(maxT - 1)){
    R[i,t] ~ dpois(theta[i]*days[i,t])
}
# Linear model for theta.
theta[i] = exp(theta00            *   gridCovariates[i,1]  +
                beta_northing      *   gridCovariates[i,2]  +
                beta_easting       *   gridCovariates[i,3]  +
                beta_elev          *   gridCovariates[i,4]  +
                beta_highway       *   gridCovariates[i,5]  +
                beta_minor_road    *   gridCovariates[i,6]  +
                beta_hab_softwood  *   gridCovariates[i,7]  +
                beta_hab_hardwood  *   gridCovariates[i,8]  +
```

```
                    beta_hab_mixed     *   gridCovariates[i,9]  +
                    beta_hab_wetland   *   gridCovariates[i,10]
    )

    # Mechanism for scat removals/deposition
    for(t in 2:maxT){
        N[i,t,1] = N[i,t-1,maxV] - y[i,t-1,maxV] + R[i,t-1]
        for(v in 2:maxV){
            N[i,t,v] = N[i,t,v-1] - y[i,t,v-1]
        }
    }

    # Observation likelihood.
    for(t in 2:maxT){
        for(v in 1:maxV){
            # Covariates on detection
            logit(p0[i,t,v]) = pInt + Dcov[i,t-1,v]*beta_detect_dist
            p[i,t,v] = p0[i,t,v] * vis[i,t,v]
            y[i,t,v] ~ dbin(p[i,t,v], N[i,t,v])
        }
    }
}
```

E: Methodology for adaptive SCR survey of moose in the Adirondacks, NY, 2017

The adaptive SCR method developed in the main article was applied to a survey of the moose population of the Adirondack Park, New York, in 2017. The authors contracted Conservation Canines to perform sampling for moose scat, who sent five detection dogs and three dog handlers to perform the work. The survey began on June 6 2017, and ended on August 31, 2017. Prior to the arrival of the detection dog crews, each transect was flagged to provide guidance to the handlers.

Transect locations were retained from the previous year (2016) if scats were found on the transect that year; a total of 32 sites were retained from 2016. A simple random sample of new locations were generated as cluster centers for new sites. These new clusters were composed of four transects sited within the immediate area of the cluster center, with a minimum separation of approximately 2-4 km apart from the nearest neighbor. A total of 47 new transects were sited resulting in 73 transects visited in the primary sampling phase in 2017.

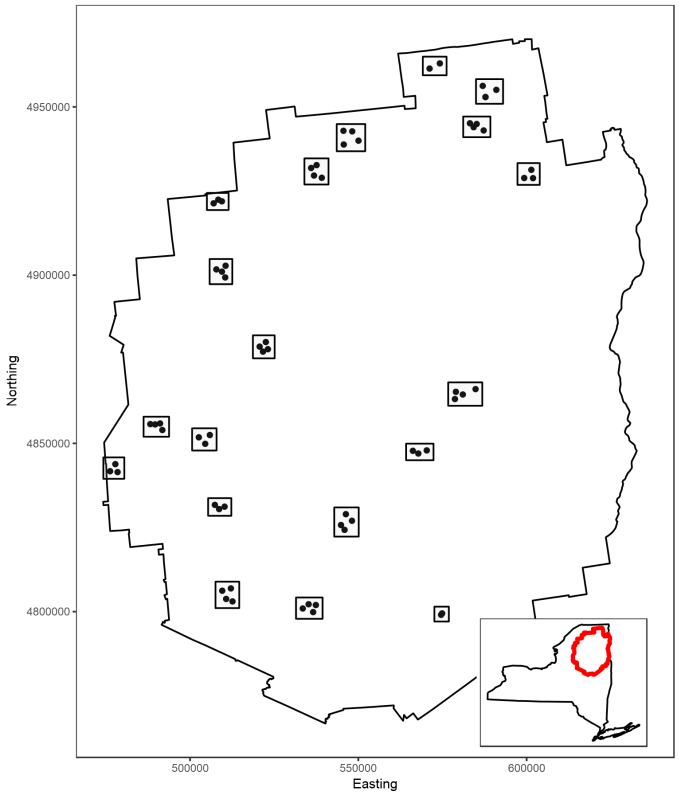

Figure 3.10: Transect locations within the Adirondack Park for the 2017 survey. Each dot represents the location of one transect, and each cluster of transects is bounded by a box. The inlaid plot indicates the extent of the Adirondack Park relative to the state of New York.

Every site was visited in the primary sampling phase to quantify the index variable – the count of scats initially found on the transect – as well as to remove as many scats as possible that existed prior to the survey. If the site had one or more scats removed from the transect in the primary phase, it was selected for re-visitation in the secondary sampling phase, making

five return visits to sample for moose scats. Thirty-nine sites had clearing counts greater than 0, and were sampled repeatedly for the remainder of the survey.

A total of 2041 scats were encountered, of which samples were taken from 1081 (the other scats were removed from the transect during the primary sampling phase). DNA extraction was performed *in situ* using cotton swabs, as well as immediately after returning home from collection in a laboratory setting. The pellets were kept frozen until their analysis by the United States Forest Service National Genomics Center for Wildlife and Fish Conservation at the Rocky Mountain Research Station (RMRS; Missoula, MT), having been shipped frozen on dry ice. The cotton swabs were kept dry in coin envelopes and also shipped to the RMRS. Analysis was completed on December 8, 2017.

A subsample of 20 scats collected during this survey were tested by the RMRS for genetic amplification by PCR. For each sample, five DNA extractions were tested with the following methods: single-pellet DNA extraction, DNA extraction from *in situ* field swabs, swab of pellet using cotton soaked with Phosphate-buffered saline (PBS) solution, and a swab using a cotton swab after soaking the pellet in PBS. All DNA extracts ($n = 139$) were tested using the following panel of microsatellite markers: RT5, RT9, RT24, RT30, BM203, BM2830, BM888, BM1225, BL42, FCB193, MAP2C, T156 and T193. There were no successful genotypes among the samples tested, and poor PCR amplicons from 14 extractions insufficient to provide a genotype.

After this result, the analysis of the remaining scat samples were halted, and we began development of the methodology described in Chapter 2.

F. Management implications of research

Successful management of the moose population in New York depends upon accurate monitoring over time. In my thesis, I provide two methodological advances that may be used with low-density species by which population is estimated by spatial capture-recapture (Chapter 1: Adaptive sampling for spatial capture-recapture), or with moose or other species by scat

surveys (Chapter 2: Quantification of moose (*Alces alces*) population from scat counts made by detection dogs).

Moose populations in Vermont and New Hampshire have experienced declines in abundance in recent years primarily due to severe infestation of ectoparasitic winter ticks (*Dermacentor albipictus*), and to a lesser extent infection by endoparasitic brain worm (*Parelaphostrongylus tenuis*) and liver fluke (*Fascioloides magna*) (Lankester 2010, Musante et al. 2010, Jones et al. 2017, Timmermann and Rodgers 2017). These infections appear to be made worse with warmer winters, which increases parasite survivorship (Murray et al. 2006). As moose are already at the southern extent of their range, climate change has the potential to reduce moose population size through mortality from a combination of parasite infection and heat stress. Moose in New York have not yet experienced the prevalence or intensity of infection of winter tick as neighboring states; it is surmised that moose densities are too low to enable epizootic events, as moose die-offs have been observed when populations exceed densities of approximately 3 moose per km^2 (Samuel 2007, Lankester 2010). Monitoring increases in the moose population may be critical in identifying potential epizootic centers should winter tick prevalence increase in the future.

Brain worm and liver fluke infection prevalence are driven by white-tailed deer (*Odocoileus virginianus*) density (Pybus 2001, Lankester 2010), and since moose are aberrant hosts, they are independent of moose density. Moose monitoring surveys utilizing the enhanced scat survey method developed in the main article can at the same time, and with little marginal cost, assess concurrent deer population densities under the same protocol, although the relatively immense number of deer fecal groups will preclude the use of detection dogs and warrant potential restriction of survey units. Unlike distance sampling, the minimum data to be collected is a spatial location, so the spatial scale of observation may be widely expanded due to the gained efficiency in the simpler data collection. Nevertheless, it would be beneficial to collect deer samples for parasite assessment. Including these data in moose monitoring surveys can help evaluate if the cause of future declines is due to apparent competition with

white-tailed deer.

Changing climate conditions have additional effects on moose that may alter their population patterns. Winters have been becoming warmer in the northeastern U.S.A., coinciding with a reduction in snowpack that will allow moose to access more forage resources in the winter than previously (Hayhoe et al. 2007, Christenson et al. 2008). However, thermal stress may cause moose to lose mass and reduce foraging during hot summers (Renecker and Hudson 1986, Rodenhouse et al. 2009), and cause a change in habitat selection (van Beest et al. 2012, Melin et al. 2014). The model developed accommodates spatial covariates easily for the purposes of testing hypotheses related to spatial changes in climate or identification of shifting patterns in selection of habitat for effective management of moose resources.

Early detection of moose population changes in New York will require a simple, inexpensive method for population assessment that can be used frequently, which the enhanced scat surveys of the second chapter provide. At a minimum, there is no collection of samples, and no genetic analyses to perform, providing excellent cost efficiency in obtaining a population estimate. The survey may be implemented in any season and in any environment where scat may accumulate, as it is unrestricted from assumptions of seasonal movement patterns of moose, and not inhibited by visual obstruction of the targets. There is no need to clear transects or plots, and so the theoretical minimum number of visits to any particular survey units is one, but estimation of scat accumulation rates are much improved with two or more visits. We emphasize the use of detection dog units because datasets are liable to be too sparse under human observation at current scat densities, and the assumptions of the observation model do not fit with the human observation process – this is better represented through distance sampling.

The method should be improved through protocol. Identification of process parameter values relies on being able to determine the rate of detection, and this is best measured through repeated sampling of areas, as we described in the development of the model. Deliberate and random replication of observation would provide a more robust estimate of detection

probability, since we cannot verify that grid cells replicated in the 2016 survey were done so independent of scat presence. We recommend linear transects that are walked twice, once to the end and back, offering replication at all grid cells visited, providing increased quality of data for estimating p. With regards to spatial design, the model does not necessarily benefit from clustering of the transects, which was a result of designing for spatial capture-recapture, but survey efficiency is greater when there are two transects together, such that the observers minimize travel time between transects. The transect siting should have an emphasis on sampling the gradient of covariates in a representative fashion. We recommend a stratified random sample for placing pairs of transects.

G. Distribution of replicated observations

A simulation study was performed to asses the ability of the model in Chapter 2 to estimate model parameters – this study led to the application of the model to the 2016 moose data. A key result of the study was that a minimum of approximately 25% of grid cells required replicate observations, two times or more. In Table 3.2, we show that the distribution of the dogs' observations of grid cells fulfills this requirement for adequate estimation of model parameters – we replicated observation of grid cells twice or more in 37% of grid cells, within any occasion v.

Table 3.2: Frequency of replication of observation of grid cells. The majority of grid cells were observed only a single time during any occasion v. Approximately 37% of grid cells were observed twice or more. Replication of approximately 6 or greater is likely an artifact of GPS error, or during rest periods when the handler would play with the dogs, involving back-and-forth movement that could produce high replicated observations.

Grid cell replication	Frequency
1	15092
2	5216
3	1948
4	860
5	403
6	190
7	114
8	71
9	38
10	13
11	12
12	12
13	10
14	6
15	4
16	1
17	1
18	1
19	1
20	1

REFERENCES

Barry, S. C., and A. H. Welsh. 2002. Generalized additive modelling and zero inflated count data. Ecological Modelling 157:179–188.

Bartzke, G. S., R. May, E. J. Solberg, C. M. Rolandsen, and E. Røskaft. 2015. Differential barrier and corridor effects of power lines, roads and rivers on moose (*Alces alces*) movements. Ecosphere 6:art67.

Bishop, M. D., S. M. Kappes, J. W. Keele, R. T. Stone, S. L. F. Sunden, G. A. Hawkins, S. S. Toldo, R. Fries, M. D. Grosz, J. Yoo, and C. W. Beattie. 1994. A genetic linkage map for cattle. Genetics 136:619–639.

Blanc, L., E. Marboutin, S. Gatti, and O. Gimenez. 2013. Abundance of rare and elusive species: Empirical investigation of closed versus spatially explicit capture-recapture models with lynx as a case study. Journal of Wildlife Management 77:372–378.

Brinkman, T. J., M. K. Schwartz, D. K. Person, K. L. Pilgrim, and K. J. Hundertmark. 2010. Effects of time and rainfall on PCR success using DNA extracted from deer fecal pellets. Conservation Genetics 11:1547–1552.

Brown, J. A. 2003. Designing an efficient adaptive cluster sample. Environmental and Ecological Statistics 10:95–105.

Brown, J. A., M. Salehi M., M. Moradi, B. Panahbehagh, and D. R. Smith. 2013. Adaptive survey designs for sampling rare and clustered populations. Mathematics and Computers in Simulation 93:108–116.

Buckland, S. T., D. A. Anderson, K. P. Burnham, and J. L. Laake. 1993. Distance Sampling: estimating the abundance of biological populations. Pages 295–349. Chapman & Hall,

London.

Bureau, U. C. 2017. 2017 tiger/line shapefiles (machine-readable data files).

Chandler, R. B., and J. A. Royle. 2013. Spatially explicit models for inference about density in unmarked or partially marked populations. Annals of Applied Statistics 7:936–954.

Christenson, L. M., D. M. J. Mitchell, and P. M. Groffman. 2008. The biogeochemistry of moose and soil freezing: multiple interactions influence on nitrogen cycling in a northern hardwood forest. PhD thesis, State University of New York College of Environmental Science; Forestry.

Christman, M. C., and F. Lan. 2001. Inverse Adaptive Cluster Sampling. Source: Biometrics 57:1096–1105.

Conn, P. B., J. T. Thorson, and D. S. Johnson. 2017. Confronting preferential sampling when analysing population distributions: diagnosis and model-based triage. Methods in Ecology and Evolution 8:1535–1546.

Conroy, M. J., J. P. Runge, R. J. Barker, M. R. Schofield, and C. J. Fonnesbeck. 2008. Efficient Estimation of Abundance for Patchily Distributed Populations Via Two-Phase, Adaptive Sampling. Ecology 89:3362–3370.

Crum, N., A. K. Fuller, C. S. Sutherland, E. G. Cooch, and J. Hurst. 2017. Estimating Occupancy Probability of Moose Using Hunter Survey Data 81:521–534.

de Valpine, P., D. Turek, C. Paciorek, C. Anderson-Bergman, D. Temple Lang, and Bodik. 2017. Programming with models: Writing statistical algorithms for general model structures with NIMBLE. Journal of Computational and Graphical Statistics 26:403–417.

Diggle, P. J., and R. Menezes. 2010. Geostatistical inference under preferential sampling:191–232.

Dussault, C., J.-P. Ouellet, C. Laurian, R. Courtois, M. Poulin, and L. Breton. 2007. Moose movement rates along highways and crossing probability models. The Journal of Widllife

Management 71:2338–2345.

Efford, M. 2004. Density estimation in live-trapping studies. Oikos 106:598–610.

Feree, C., and M. Anderson. 2013. A map of terrestrial habitats of the northeastern united states: Methods and approach. The Nature Conservancy, Eastern Conservation Science, Eastern Regional Office, Boston, MA.

Frair, J. 2017.. personal communication.

Gardner, B., J. Reppucci, M. Lucherini, and J. A. Royle. 2010. Spatially explicit inference for open populations: Estimating demographic parameters from camera-trap studies. Ecology 91:3376–3383.

Geiger, R., R. H. Aron, and P. Todhunter. 1995. The Climate Near the Ground. Fifth editions. Harvard University Press, Cambridge.

Hayhoe, K., C. P. Wake, T. G. Huntington, L. Luo, M. D. Schwartz, J. Sheffield, E. Wood, B. Anderson, J. Bradbury, A. DeGaetano, T. J. Troy, and D. Wolfe. 2007. Past and future changes in climate and hydrological indicators in the US Northeast. Climate Dynamics 28:381–407.

Hickey, L. 2008. Assessing re-colonization of moose in New York with HSI models. Alces 44:117–126.

Jenkins, K. J., and B. F. J. Manly. 2008. A double-observer method for reducing bias in faecal pellet surveys of forest ungulates. Journal of Applied Ecology 45:1339–1348.

Johnson, D. S., P. B. Conn, M. B. Hooten, J. C. Ray, and B. A. Pond. 2013. Spatial occupancy models for large data sets. Ecology 94:801–808.

Jolly, G. 1965. Explicit estimates from capture-recapture data with both death and immigration-stochastic model. Biometrika 52:225–247.

Jones, H., P. J. Pekins, L. E. Kantar, M. O'Neil, and D. Ellingwood. 2017. Fecundity and summer calf survival of moose during 3 successive years of winter tick epizootics. Alces

53:85–98.

Joyal, R., and J.-G. Richard. 1986. Winter defecation output and bedding frequency of wild, free-ranging moose. Journal of Wildlife Management 50:734–736.

Kéry, M., and J. A. Royle. 2015. Applied Hierarchical Modeling in Ecology: Analysis of distribution, abundance and species richness in R and BUGS: Volume 1: Prelude and Static Models. Academic Press.

Kéry, M., B. Gardner, T. Stoeckle, D. Weber, and J. A. Royle. 2011. Use of Spatial Capture-Recapture Modeling and DNA Data to Estimate Densities of Elusive Animals. Conservation Biology 25:356–364.

Kéry, M., J. A. Royle, H. Schmid, M. Schaub, B. Volet, G. Häfliger, and N. Zbinden. 2010. Site-Occupancy Distribution Modeling to Correct Population-Trend Estimates Derived from Opportunistic Observations. Conservation Biology 24:1388–1397.

Kohn, M. H., E. C. York, D. A. Kamradt, G. Haught, R. M. Sauvajot, and R. K. Wayne. 1999. Estimating population size by genotyping faeces. Proceedings of the Royal Society B: Biological Sciences 266:657–663.

Kretser, H., M. Glennon, A. Whitelaw, A. Hurt, K. Pilgrim, and M. Schwartz. 2016. Scat-Detection Dogs Survey Low Density Moose in New York. Alces 52:55–66.

Laing, S. E., S. T. Buckland, R. W. Burn, D. Lambie, and A. Amphlett. 2003. Dung and nest surveys: Estimating decay rates. Journal of Applied Ecology 40:1102–1111.

Lankester, M. W. 2010. Understanding the impact of meningeal worm, *Parelaphostrongylus tenuis*, on moose populations. Alces 46:53–70.

Laurian, C., C. Dussault, J.-P. Ouellet, R. Courtois, and M. Poulin. 2012. Interactions between a large herbivore and a road network. Ecoscience 19:69–79.

Long, R. A., T. M. Donovan, P. Mackay, W. J. Zielinski, and J. S. Buzas. 2007. Effectiveness of scat detection dogs for detecting forest carnivores. Journal of Wildlife Management

71:2007–2017.

MacCracken, J. G., and V. V. Ballenberge. 1987. Age- and sex-related differences in fecal pellet dimensions of moose. The Journal of Wildlife Management 51:360.

Marques, F. F. C., S. T. Buckland, D. Goffin, C. E. Dixon, D. L. Borchers, B. A. Mayle, and A. J. Peace. 2001. Estimating deer abundance from line transect surveys of dung: Sika deer in southern Scotland. Journal of Applied Ecology 38:349–363.

Martin, T. G., B. A. Wintle, J. R. Rhodes, P. M. Kuhnert, S. A. Field, S. J. Low-Choy, A. J. Tyre, and H. P. Possingham. 2005. Zero tolerance ecology: Improving ecological inference by modelling the source of zero observations. Ecology Letters 8:1235–1246.

Maudet, C., G. Luikart, D. Dubray, A. Von Hardenberg, and P. Taberlet. 2004. Low genotyping error rates in wild ungulate faeces sampled in winter. Molecular Ecology Notes 4:772–775.

McCann, N. 2013. Warm-season heat stress in moose (*Alces alces*). Canadian Journal of Zoology 898:893–898.

Melin, M., J. Matala, L. Mehtätalo, R. Tiilikainen, O. P. Tikkanen, M. Maltamo, J. Pusenius, and P. Packalen. 2014. Moose (Alces alces) reacts to high summer temperatures by utilizing thermal shelters in boreal forests - an analysis based on airborne laser scanning of the canopy structure at moose locations. Global Change Biology 20:1115–1125.

Miquelle, D. 1983. Summer Defecation-Urination Rates and Volumes of Moose. Journal of Wildlife Management 47:1230–1233.

Morrison, M., W. M. Block, M. D. Strickland, and W. L. Kendall. 2001. Wildlife Study Design. (D. E. Alexander, Ed.). Springer, New York.

Murphy, M. A., L. P. Waits, and K. C. Kendall. 2003. The influence of diet on faecal DNA amplification and sex identification in brown bears (Ursus arctos). Molecular Ecology

12:2261–2265.

Murray, D. L., E. W. Cox, W. B. Ballard, H. A. Whitlaw, M. S. Lenarz, T. W. Custer, T. Barnett, and T. K. Fuller. 2006. Pathogens, nutritional deficiency, and climate influences on a declining moose population. Wildlife Monographs 166:1–30.

Musante, A. R., P. J. Pekins, and D. L. Scarpitti. 2010. Characteristics and dynamics of a regional moose *Alces alces* population in the northeastern United States. Wildlife Biology 16:185–204.

Pacifici, K., R. M. Dorazio, and M. J. Conroy. 2012. A two-phase sampling design for increasing detections of rare species in occupancy surveys. Methods in Ecology and Evolution 3:721–730.

Pacifici, K., B. J. Reich, R. M. Dorazio, and M. J. Conroy. 2016. Occupancy estimation for rare species using a spatially-adaptive sampling design. Methods in Ecology and Evolution 7:285–293.

Palsboll, P. J. 1999. Genetic tagging: contemporary molecular ecology. Biol. J Linn. Soc. 68:3–22.

Pati, D., B. Reich, and D. Dunson. 2011. Bayesian geostatistical modelling with informative sampling locations. Biometrika 98:35–48.

Peek, J. M., D. L. Ulrich, and R. J. Mackie. 1976. Moose habitat selection and relationships to forest management in nortestern Minnesota. Wildlife Monographs 1976:3–65.

Plummer, M. 2017. JAGS: Just another gibbs sampler. http://mcmc-jags.sourceforge.net.

Pollock, K. H. 1991. Modeling capture, recapture and removal statistics for estimation of demographic parameters for fish and wildlife productions: past, present and future. Journal of the American Statistical Association 86:225–235.

Pybus, M. 2001. Parasitic Diseases of Wild Mammals. Pages 357–364 (W. M. Samuel, M. J.

Pybus, and A. A. Kocan, Eds.). Iowa State University Press, Ames, Iowa.

R Core Team. 2017. R: A language and environment for statistical computing. Vienna, Austria.

Rapley, V. E., and A. H. Welshy. 2008. Model-based inferences from adaptive cluster sampling. Bayesian Analysis 3:717–736.

Rådström, P., R. Knutsson, and P. Wolffs. 2004. Pre-PCR Processing. Molecular microbiotechnology 26:133–146.

Renecker, L. A., and R. J. Hudson. 1986. Seasonal energy expenditures and thermoregulatory responses of moose. Canadian Journal of Zoology 64:322–327.

Rodenhouse, N. L., L. M. Christenson, D. Parry, and L. E. Green. 2009. Climate change effects on native fauna of northeastern forests. Canadian Journal of Forest Research 39:249–263.

Royle, J. A., and S. J. Converse. 2014. Hierarchical spatial capture-recapture models: Modelling population density in stratified populations. Methods in Ecology and Evolution 5:37–43.

Royle, J. A., and R. M. Dorazio. 2012. Parameter-expanded data augmentation for Bayesian analysis of capture-recapture models. Journal of Ornithology 152:521–537.

Royle, J. A., R. B. Chandler, R. Sollmann, and B. Gardner. 2014a. Spatial Capture-Recapture. Page iii. Elsevier Inc, Waltham, MA.

Royle, J. A., R. B. Chandler, C. C. Sun, and A. K. Fuller. 2014b. Reply to Efford on 'Integrating resource selection information with spatial capture-recapture'. Methods in Ecology and Evolution 5:603–605.

Royle, J. A., S. J. Converse, and W. A. Link. 2012. Data Augmentation for Hierarchical Capture-recapture Models:1–19.

Royle, J. A., A. K. Fuller, and C. Sutherland. 2018. Unifying population and landscape

ecology with spatial capture–recapture. Ecography 41:444–456.

Rue, H., S. Martino, and N. Chopin. 2009. Approximate Bayesian inference for latent Gaussian models by using integrated nested Laplace approximations. Journal of the royal statistical society: Series b (statistical methodology) 71:319–392.

Salehi, M., and G. A. Seber. 1997. Two-Stage Adaptive Cluster Sampling. Biometrics 53:959–970.

Salehi, M., and G. A. F. Seber. 2002. Unbiased Estimators for Restricted Adaptive Cluster Sampling. Aust. N. Z. J. Stat 44:63–74.

Samuel, W. M. 2007. Factors affecting epizootics of winter ticks and mortality of moose. Alces 43:39–48.

Seber, G. A. F., and C. J. Schwarz. 1999. Estimating animal abundance: review III. Statistical Science 14:427–456.

Smith, D. A., K. Ralls, A. Hurt, B. Adams, M. Parker, B. Davenport, M. C. Smith, and J. E. Maldonado. 2003. Detection and accuracy rates of dogs trained to find scats of San Joaquin kit foxes (*Vulpes macrotis mutica*). Animal Conservation 6:339–346.

Smith, D. R., Y. Lei, C. A. Walter, and J. A. Young. 2012. Incorporating predicted species distribution in adaptive and conventional sampling designs. Pages 381–396 *in* R. Gitzen, J. Millspaugh, A. Cooper, and D. Licht, editors. Design and analysis of long-term ecological monitoring studies. Cambridge University Press.

Sollmann, R., N. M. Tôrres, M. M. Furtado, A. T. De Almeida Jácomo, F. Palomares, S. Roques, and L. Silveira. 2013. Combining camera-trapping and noninvasive genetic data in a spatial capture-recapture framework improves density estimates for the jaguar. Biological Conservation 167:242–247.

Street, G. M., L. M. Vander Vennen, T. Avgar, A. Mosser, M. L. Anderson, A. R. Rodgers, and J. M. Fryxell. 2015. Habitat selection following recent disturbance: model transferability

with implications for management and conservation of moose (*Alces alces*). Canadian Journal of Zoology 93:813–821.

Sun, C. C., A. K. Fuller, and J. Andrew Royle. 2014. Trap configuration and spacing influences parameter estimates in spatial capture-recapture models. PLoS ONE 9:e88025.

Survey, U. G. 2017. The national elevation dataset.

Sutherland, C., A. K. Fuller, J. A. Royle, and S. Madden. 2018. Large-scale variation in density of an aquatic ecosystem indicator species. Scientific Reports 8:1–10.

Thompson, S. K. 1990. Adaptive cluster sampling. Journal of the American Statistical Association 85:1050–1059.

Thompson, W., editor. 2013. Sampling rare or elusive species: concepts, designs, and techniques for estimating population parameters. Island Press.

Timmermann, H. R., and J. G. McNicol. 1988. Moose habitat needs. Forestry Chronicle 64:238–245.

Timmermann, H. R., and A. R. Rodgers. 2017. The status and Management of moose in North America - Circa 2015. Alces 53:1–22.

Turk, P., and J. J. Borkowski. 2005. A review of adaptive cluster sampling: 1990-2003. Environmental and Ecological Statistics 12:55–94.

van Beest, F. M., B. Van Moorter, and J. M. Milner. 2012. Temperature-mediated habitat use and selection by a heat-sensitive northern ungulate. Animal Behaviour 84:723–735.

Wasser, S. K., B. Davenport, E. R. Ramage, K. E. Hunt, M. Parker, C. Clarke, and G. Stenhouse. 2004. Scat detection dogs in wildlife research and management: application to grizzly and black bears in the Yellowhead Ecosystem, Alberta, Canada. Canadian Journal of Zoology 82:475–492.

Wasser, S. K., C. S. Houston, G. M. Koehler, G. G. Cadd, and S. R. Fain. 1997. Techniques for

application of faecal DNA methods to field studies of Ursids. Molecular Ecology 6:1091–1097.

Wattles, D. W., and S. DeStefano. 2011. Status and management of moose in the Northeastern United States. Alces 47:53–68.

Welsh, A., R. Cunningham, C. Donnelly, and D. Lindenmayer. 1996. Modelling the abundance of rare species: statistical models for counts with extra zeros. Ecological Modelling 88:297–308.

Williams, B. K., J. D. Nichols, and M. Conroy. 2002. Analysis and management of animal populations. Page 817. Academic Press.

Wilson, G. A., C. Strobeck, L. Wu, and J. W. Coffin. 1997. Characterization of microsatellite loci in caribou *Rangifer tarandus*, and their use in other artiodactyls. Molecular ecology 6:697–699.

Wilson, R. E., T. J. McDonough, P. S. Barboza, S. L. Talbot, and S. D. Farley. 2015. Population genetic structure of moose (*Alces Alces*) of south-central Alaska. Alces 51:71–86.

Wong, A., A. Fuller, and J. A. Royle. 2018. Adaptively sampled spatial capture recapture - simulation study. https://github.com/awong234/AdaptiveSCR.